Cell Reports

Resource

Alternative mRNA splicing events and regulators in epidermal differentiation

Graphical abstract

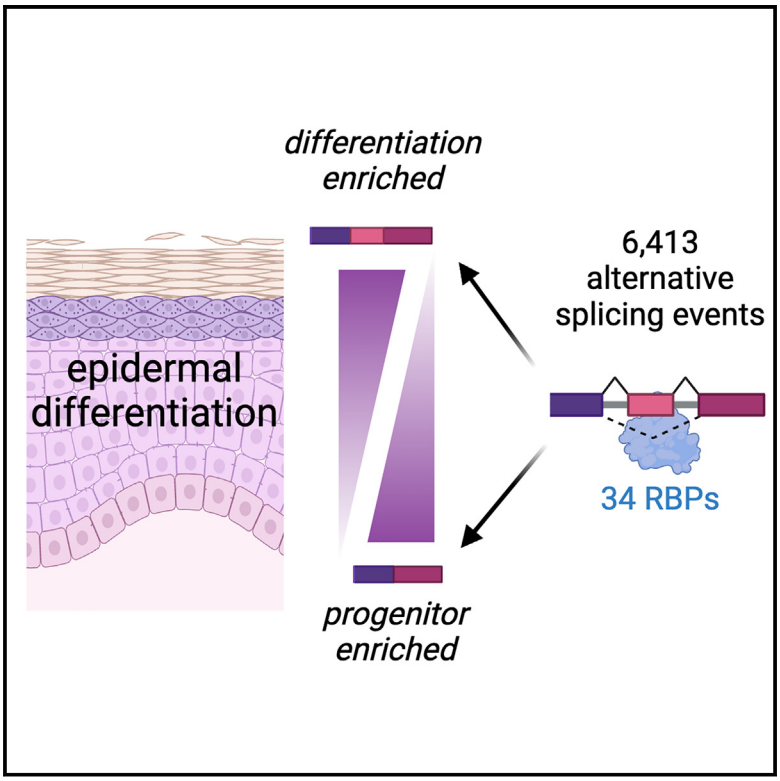

Highlights

- Epidermal differentiation is associated with 6,413 alternative mRNA splicing events
- Splicing affects signal transduction, chromatin modification, and other key processes
- Alternative splicing of a single exon of *MAP3K7* regulates epidermal differentiation

Authors

Shota Takashima, Wujianan Sun, Auke B.C. Otten, ..., Zongkai Li, Kun Qu, Bryan K. Sun

Correspondence

sunb8@hs.uci.edu

In brief

Takashima et al. demonstrate that human epidermal differentiation is associated with >6,000 alternative mRNA splicing events. Hundreds of genes undergo alternative splicing without substantial changes to steady-state expression. One such splicing event, involving alternative inclusion of a single exon of *MAP3K7*, controls the differentiation of epidermal keratinocytes.

Takashima et al., 2024, Cell Reports *43*, 113814
March 26, 2024
https://doi.org/10.1016/j.celrep.2024.113814

CellPress

Cell Reports

CellPress
OPEN ACCESS

Resource

Alternative mRNA splicing events and regulators in epidermal differentiation

Shota Takashima,[1,4] Wujianan Sun,[2,4] Auke B.C. Otten,[1] Pengfei Cai,[2] Shaohong Isaac Peng,[1] Elton Tong,[1] Jolina Bui,[1] McKenzie Mai,[1] Oyumergen Amarbayar,[1] Binbin Cheng,[1] Rowen Jane Odango,[1] Zongkai Li,[2] Kun Qu,[2] and Bryan K. Sun[1,3,5,*]

[1]Department of Dermatology, University of California San Diego, La Jolla, CA 92109, USA
[2]Department of Oncology, The First Affiliated Hospital of USTC, School of Basic Medical Sciences, Division of Life Sciences and Medicine, University of Science and Technology of China, Hefei 230027, China
[3]Present address: Department of Dermatology, University of California Irvine, Irvine, CA 92697, USA
[4]These authors contributed equally
[5]Lead contact
*Correspondence: sunb8@hs.uci.edu
https://doi.org/10.1016/j.celrep.2024.113814

SUMMARY

Alternative splicing (AS) of messenger RNAs occurs in ~95% of multi-exon human genes and generates diverse RNA and protein isoforms. We investigated AS events associated with human epidermal differentiation, a process crucial for skin function. We identified 6,413 AS events, primarily involving cassette exons. We also predicted 34 RNA-binding proteins (RBPs) regulating epidermal AS, including 19 previously undescribed candidate regulators. From these results, we identified FUS as an RBP that regulates the balance between keratinocyte proliferation and differentiation. Additionally, we characterized the function of a cassette exon AS event in *MAP3K7*, which encodes a kinase involved in cell signaling. We found that a switch from the short to long isoform of *MAP3K7*, triggered during differentiation, enforces the demarcation between proliferating basal progenitors and overlying differentiated strata. Our findings indicate that AS occurs extensively in the human epidermis and has critical roles in skin homeostasis.

INTRODUCTION

Alternative splicing (AS) is a process in which multiple mRNA and protein isoforms are generated from the use of different splice sites on a pre-messenger RNA. Up to 95% of human multi-exon genes undergo AS,[1] but it is unclear how many AS events are biologically functional.[2,3] Cross-species and tissue comparisons show that many AS events occur within a single organ,[4] consistent with reports describing functions for AS in the brain,[5] muscle,[6] and other tissues.[7] These findings indicate that AS has major biological roles in tissue-specific processes. However, gene and protein expression databases do not always discriminate the relative expression of different isoforms between cell states or cell types within an organ.[4,8] Therefore, we have an incomplete understanding of the potential role of AS in processes such as tissue homeostasis and cellular differentiation.

The epidermis is a self-renewing epithelium consisting principally of stratified layers of keratinocytes. The innermost layer contains stem/progenitor keratinocytes that can either replicate within the basal layer or detach from the basement membrane and migrate upwards into suprabasal layers. As keratinocytes move superficially, they progressively differentiate and express proteins that provide mechanical strength and establish the skin's functional barrier. The identity of genes and epigenetic events that orchestrate the switch from progenitor to differentiated layers of epidermis have been reported,[9,10] but we do not understand the full extent to which AS influences this process. Critical regulators including *TP63*,[11] *DMKN*,[12] and *ECM1*[13] are generated in multiple isoforms that have distinct functions in the skin. Additionally, RNA-splicing-associated proteins such as *ESRP1*,[14] *ESRP2*,[14] and *ZMAT2*[15] are essential to epidermal function. These examples demonstrate a role for AS in maintaining human epidermis and underscore the value of defining the full repertoire of AS events and their regulators in the skin.

In this study, we determined the total and relative expression of mRNA isoforms in stem/progenitor and differentiated primary human epidermal keratinocytes. We found that epidermal differentiation is associated with thousands of AS events. We performed binding motif analysis to identify candidate RNA-binding factors that mediate epidermal AS and demonstrated the use of this candidate list to identify functional epidermal RNA-binding proteins (RBPs). Finally, we investigated a previously unstudied epidermal AS event to demonstrate the potential application of the AS dataset. The results indicate that thousands of AS events are associated with epidermal differentiation and serve as a resource to study the roles of specific AS events regulating this process.

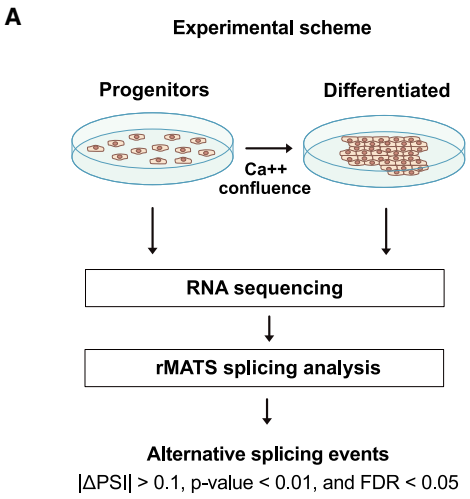

B

Alternative splicing events in human keratinocytes

Alternative splicing event	Prog	Diff	Total
Skipped exon SE	1860	1977	3837
Alternative 3' splice site A3SS	297	160	457
Alternative 5' splice site A5SS	266	153	419
Mutually exclusive exon MXE	490	557	1047
Retained intron RI	486	167	653
Total	3014	3399	6413

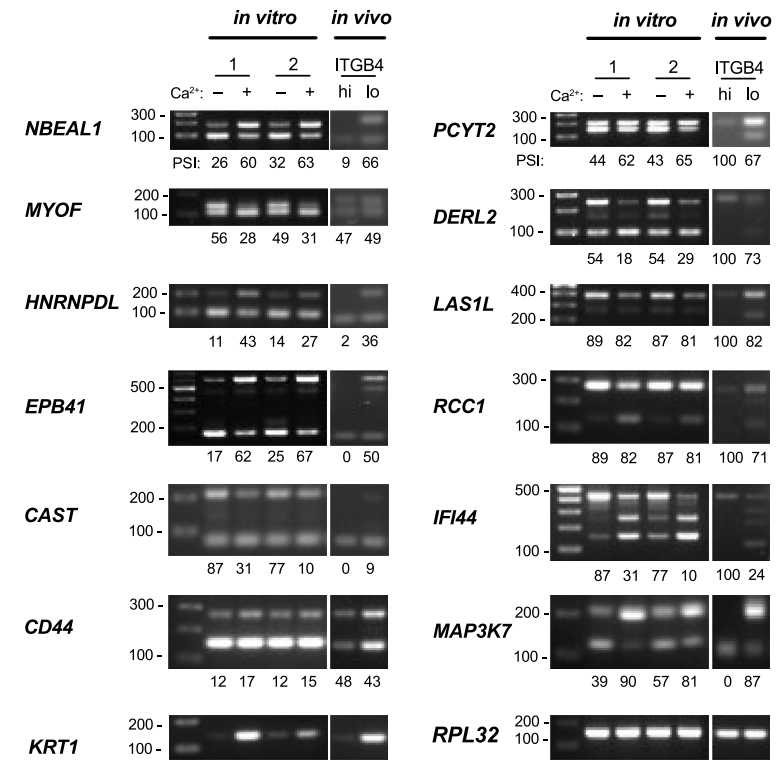

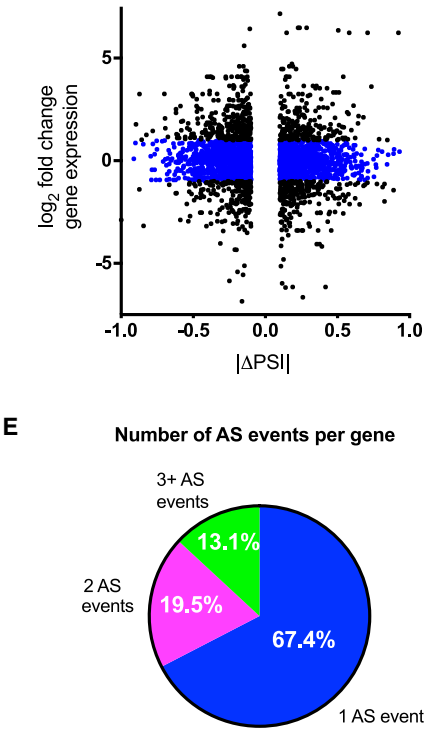

Figure 1. Alternative mRNA splicing events in human epidermal differentiation

(A) Experimental design to identify mRNA splicing isoforms in progenitor and differentiated epidermal keratinocytes.

(B) Number and type of alternative mRNA splicing events in progenitor and differentiated human epidermal keratinocytes. The full list of splicing events is listed in Table S1.

(C) RT-PCR of alternatively spliced skipped exon (SE) events identified by rMATS. PSI, percent spliced in, represented by percentage of exon-included isoform. *In vitro* columns show primary keratinocytes differentiated in cell culture by confluent growth conditions with supplemented calcium (Ca^{2+}). 1 and 2 represent biological replicates. *In vivo* columns show epidermal keratinocytes flow sorted from intact truncal skin of an adult male into beta 4 integrin (ITGB4) high and low populations. KRT1 (keratin 1) is a differentiation-specific transcript control; RPL32 is a ribosomal protein transcript invariant control.

(legend continued on next page)

RESULTS

Thousands of alternative mRNA splicing events in epidermal differentiation

We performed 150-nucleotide paired-end whole-transcriptome sequencing of total RNA isolated from primary neonatal human epidermal keratinocytes cultured in progenitor and differentiated states (n = 3 each) (Figure 1A). Experimental induction of keratinocyte differentiation was verified by downregulation of progenitor-associated genes and upregulation of differentiation-associated genes (Figure S1). Distance heatmaps and principal-component analysis confirmed the grouping of progenitor and differentiated transcriptomes (Figure S1). Transcriptomes were analyzed with rMATS,[16] a model designed to measure AS.

Differential splicing can be quantitated by the difference in the inclusion of the alternatively spliced region as "percent spliced in," or ΔPSI. We chose the criteria of |ΔPSI| >0.1, a p value of <0.01, and a false discovery rate (FDR) <0.05 as a threshold to define an AS event. This threshold was selected to be permissive based on the intent to generate a discovery dataset. Based on these criteria, we identified 6,413 AS events that were characteristic of either the epidermal progenitor or differentiated state (Figure 1B; Table S1). Applying more stringent criteria by lowering the FDR and/or increasing the |ΔPSI| threshold reduced the number of called events, as expected (Figure S2). However, even filtering for AS events with large magnitude changes (|ΔPSI| > 0.4) and a stringent FDR (<0.001) identified 408 skipped exon (SE) events, suggesting that AS is prevalent during epidermal keratinocyte differentiation.

AS events can be classified by the characteristics of the alternatively spliced region. The inclusion or exclusion of an exon is designated a SE, also known as a cassette exon. The use of different 5′ or 3′ splice sites classifies alternative 5′ or 3′ splice sites, while the inclusion of two distinct intervening exons in different isoforms classifies mutually exclusive exons. The absence of splicing across consecutive intron-exon junctions designates a retained intron (RI). SE events were the predominant type of AS event, accounting for 3,837 (~60%) of all events (Figure 1B). The predominance of SE-type events is consistent with AS studies in other tissues and organisms and is postulated to reflect the global biological importance of SE-type events.[17] Because of the overrepresentation of SEs in this dataset and their historical focus in the study of other tissues and species, we focus our subsequent analyses on SE events.

To assess the potential physiological relevance of these AS events, we examined the number of AS events affecting genes belonging to a core gene set linked to keratinocyte cell-fate decisions.[18] We identified 68 AS events affecting these pivotal genes (Table S3), indicating that AS occurs in epidermal regulatory genes. Next, we explored the potential disease relevance of the AS dataset by comparing it to splicing events associated with psoriasis. Psoriasis is a common, debilitating skin disease characterized by epidermal hyperproliferation and impaired differentiation. We performed rMATS splicing analysis on 92 psoriasis and 82 control RNA sequencing (RNA-seq) samples (NIH GEO: GSE54456) and identified 133 AS events affecting 89 genes associated with psoriasis that intersected with our AS dataset (Table S4). We propose these AS events and genes as high-value candidates to explore for having potential roles in psoriasis.

To corroborate the AS events identified by rMATS, we performed reverse transcriptase polymerase chain reaction (RT-PCR) on a sample of gene transcripts predicted to have multiple isoforms. We selected a sample of 12 genes, including examples of genes in the core epidermal and psoriasis gene sets (*LAS1L*, *IFI44*, *CD44*, *RCC1*), genes predicted to switch to either the longer or shorter isoform upon differentiation, as well as transcripts with >2 isoforms (Figure 1C). Additionally, to evaluate if the isoforms identified *in vitro* were also expressed *in vivo*, we also performed RT-PCR on cells isolated from human epidermal tissue and partitioned by flow sorting (Figure S1) by integrin beta 4 (ITGB4). ITGB4 expression is specific to keratinocytes in the basal layer, which we leveraged to enrich for progenitor (ITGB4 high) vs. differentiated (ITGB4 low) keratinocytes.

RT-PCR showed that all 12 tested genes displayed the expected mRNA isoforms identified by rMATS in *in-vitro*- and *in-vivo*-derived RNA (Figure 1C). Relative ratios of isoform expression in progenitor vs. differentiated states were concordant between *in vitro* and *in vivo* RNA in 8 of 12 tested genes, were equivocal for 2 genes, and were discordant in 2 genes. Collectively, these results indicated that the rMATS sequencing analysis applied to *in vitro* primary keratinocyte RNA identified epidermal mRNA transcript isoforms expressed *in vivo*. Relative isoform expression changes observed during *in vitro* differentiation agreed often, but not always, with the patterns observed in epidermal tissue *in vivo*.

We and others have profiled the dynamic gene expression changes that occur during epidermal differentiation.[9,10,19] However, AS can alter gene function without affecting steady-state mRNA levels. We examined the relationship between epidermal genes undergoing AS and their overall mRNA expression level. We found that 1,319 AS events occurred in 849 genes, whose overall expression differed by less than 2-fold when comparing progenitors with differentiated cells (Figure 1D; Table S1). These genes included well-known epidermal regulators *CTNND1*,[20] *AKT2*,[21] and *IKBKG*,[22] whose perturbations cause mouse and/or human skin disease phenotypes. These results demonstrated that a substantial fraction of epidermal AS events occur without major changes to overall steady-state mRNA levels.

Multiple AS events can occur within the same gene and transcript. In our AS dataset, we found that 67.4% of AS events were the only predicted AS events in that transcript. By contrast, 19.5% of gene transcripts had two distinct AS events, and 13.1% had three or more AS events (Figure 1E). These results illustrate the potential combinatorial complexity from AS in epidermal genes.

(D) Scatterplot showing magnitude of alternative splicing (AS) change (ΔPSI) vs. expression level for epidermal gene transcripts when comparing progenitor vs. differentiated keratinocytes. Blue dots represent transcripts displaying greater than 10% splicing isoform differences (|ΔPSI|>0.1) and <2-fold total gene expression change.
(E) Proportion of distinct AS events in epidermal genes.

Characteristics of SE AS events in epidermal keratinocytes

The number of AS events resulting in increased or decreased cassette exon inclusion was comparable between progenitor and differentiated keratinocytes (Figure 2A). Gene Ontology (GO) analysis of progenitor AS events identified enrichment in genes associated with organelle assembly, histone acetylation, and phosphorylation (Figure 2B). In differentiated keratinocytes, ontology analysis highlighted genes associated with histone modification, nuclear export, and regulation of RNA splicing.

The inclusion of a cassette exon can lead to an in-frame insertion or a frameshift. Most epidermal AS events cause an in-frame insertion, but ~40% of epidermal AS exons result in a +1 or +2 base-pair frameshift (Figure 2C). Frameshifting exons can alter downstream peptide sequences, introduce a stop codon, and/or elicit nonsense-mediated decay.[7] The substantial fraction of splicing events predicted to generate an alternative or premature stop codon indicates the widespread potential for AS to mediate changes to peptide sequence and/or transcript stability in the epidermis.

To assess the extent of species conservation of epidermal AS events, we examined the overlap of genes displaying evidence of AS in human and mouse epidermis transcriptomes. We performed rMATS splicing analysis of an RNA-seq dataset generated from mouse embryonic and neonatal epidermis[23] (GEO: 161387). Consistent with studies that observed substantial differences in AS across different species,[24] we found that only ~10% of epidermal genes showed evidence of AS in both mouse and human epidermis (Figure 2D; Figure S1), similar to the fraction of conserved AS observed in other mouse/human comparative splicing studies.[25] Ontology analysis on conserved mouse/human AS genes in epidermal progenitors showed the strongest enrichment for genes involved with protein phosphorylation ($p < 1 \times 10^{-8}$), a biological process that appears to be disproportionately affected by splicing-mediated regulation.[26] GO analysis of differentiated AS events showed the strongest enrichment for genes involved with histone deacetylation ($p < 1 \times 10^{-5}$).

As another approach to assess the biological impact of AS events in the epidermis, we identified the protein domains affected by epidermal AS events (Figure 2E). To do so, we annotated cassette exon peptide sequences using InterPro,[27] a database of protein families and domains. We identified and counted the types of protein domains affected by epidermal SE events. Exons affected by SE in the epidermis encoded sequences for a diverse set of protein domains including Krüppel-associated boxes, GTP-binding domains, zinc-finger regions, and others. The breadth of functional domains involved with AS reflects its impact on known regulatory-type domains within epidermal gene transcripts and proteins.

RBPs in epidermal AS

AS is mediated in part by RBPs and splicing factors that assemble at regulatory sequences on the pre-mRNA. To identify candidate RBPs involved in epidermal AS, we applied MEME suite tools[28] to evaluate 300-nucleotide intervals spanning the exon-intron junctions of alternatively spliced exons (Figures 3A and 3B; Table S2). The intervals comprised 50 bp of the exon sequence and 250 bp of the adjacent intron. Applying a threshold p value <0.01 and an e value <1, MEME analysis nominated 41 RBP candidates. The candidates included factors with well-defined roles in the epidermis such as SRSF1,[29] ESRP2,[14] and YBX1.[30] Of the uncharacterized candidates, seven RBPs (A1CF, KHDRBS3, LIN28A, PABPC3, PPRC1, RBM24, and ZC3H10) had low or undetectable epidermal expression according to the Human Protein Atlas.[8] The other 34 RBPs were expressed in epidermis based on RNA and protein expression data (Figure S3). We propose these RBPs as a candidate set of regulators of SE splicing in epidermal differentiation (Table 1).

We considered if these candidate epidermal RBPs may cooperate to affect discrete biological processes. We reasoned that RBPs targeting the same set of mRNAs involved in a molecular function would reflect potential for cooperative activity. We integrated two sets of data: the expression of each RBP in progenitor/differentiated states and its predicted mRNA targets. We calculated a Pearson's correlation coefficient for expression of each RBP and the inclusion level of AS events of its target epidermal transcripts (Figure S4). After clustering the output, we observed that some RBPs such as RBM4, FUS, and PCBP1 were generally distinct from the others. On the other hand, some RBPs clustered together, including groups that had been previously reported to function cooperatively in other cell or gene contexts (e.g., YBX1 and HNRNPC[42]). We applied GO analysis to gene sets to infer potential functions associated with each RBP cluster (Figure S4). These results provide a framework to connect the epidermal RBPs (Table 1) with the biological processes impacted by epidermal SE events and suggested that RBPs may function coordinately to regulate biological processes in the epidermis.

We next explored how we could apply the RBP candidate list to identify functional epidermal RBPs. Because sequence-based motif analysis has limitations to its sensitivity and specificity,[43] we assessed our candidate list together with public RNA-protein interaction data from UV cross-linking and immunoprecipitation (CLIP) assays. Although these CLIP data were not derived from keratinocytes, RBPs frequently bind the same gene transcript in different cell types, particularly if the transcript is highly expressed.[44] Taking advantage of this observation, we evaluated RNA binding data[44] of the RBPs on our candidate list (Table 1), focusing only on binding data at intron-exon boundaries of epidermal AS transcripts. We plotted binding data for eight RBPs on our candidate list (FUS, HNRNPA1, HNRNPC, HNRNPL, KHDRBS1, SRSF1, TSRDBP, and TIA1). As a well-defined splicing regulator in keratinocytes,[29] SRSF1 served as an analytical positive control and showed robust CLIP enrichment at epidermal AS intron-exon boundaries (Figure S5). From the remaining RBPs, we selected FUS and TARDBP for further evaluation because they also showed enrichment of binding to exon/intron boundaries at epidermal AS genes.

To experimentally test the predicted binding of these RBPs to epidermal transcripts, we performed RNA immunoprecipitation for SRSF1, TARDBP, and FUS in primary keratinocytes. We assayed for the interaction with candidate epidermal RNAs in our AS dataset. Both endpoint (Figure 3C) and quantitative (Figure 3D) results showed enriched association of FUS with the predicted mRNA targets *HNRNPA1* and *DAZAP1*, as well as association of TARDBP with predicted targets *PILRB* and *PTMA*.

CellPress
OPEN ACCESS

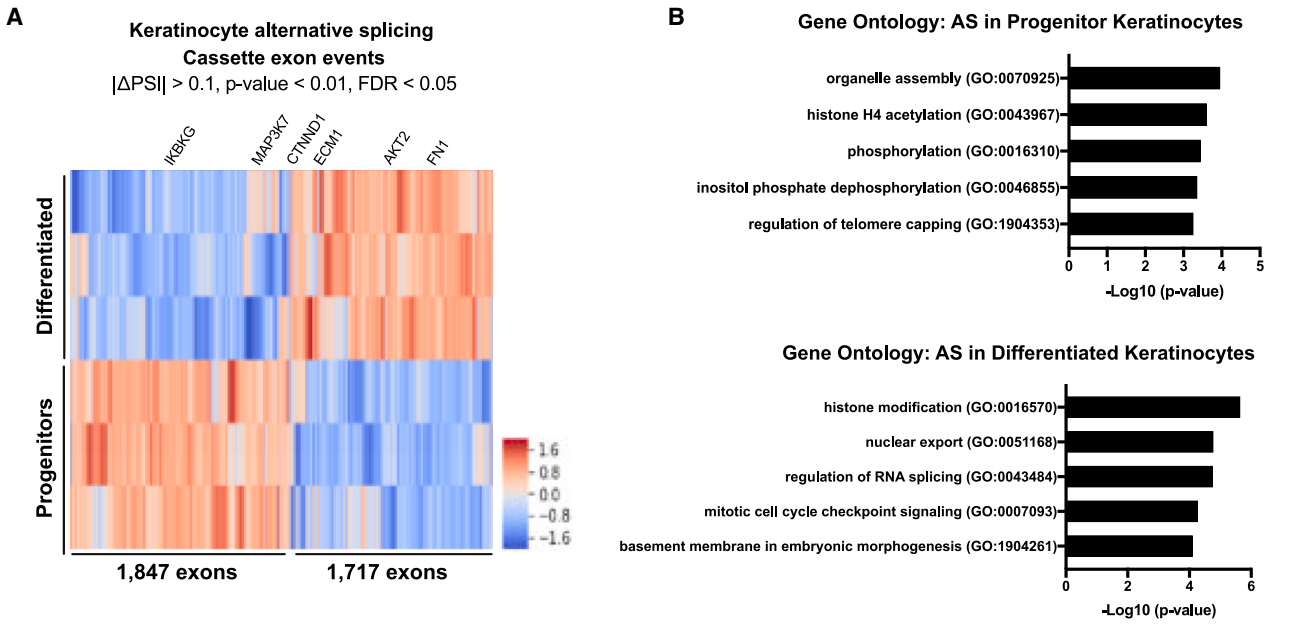

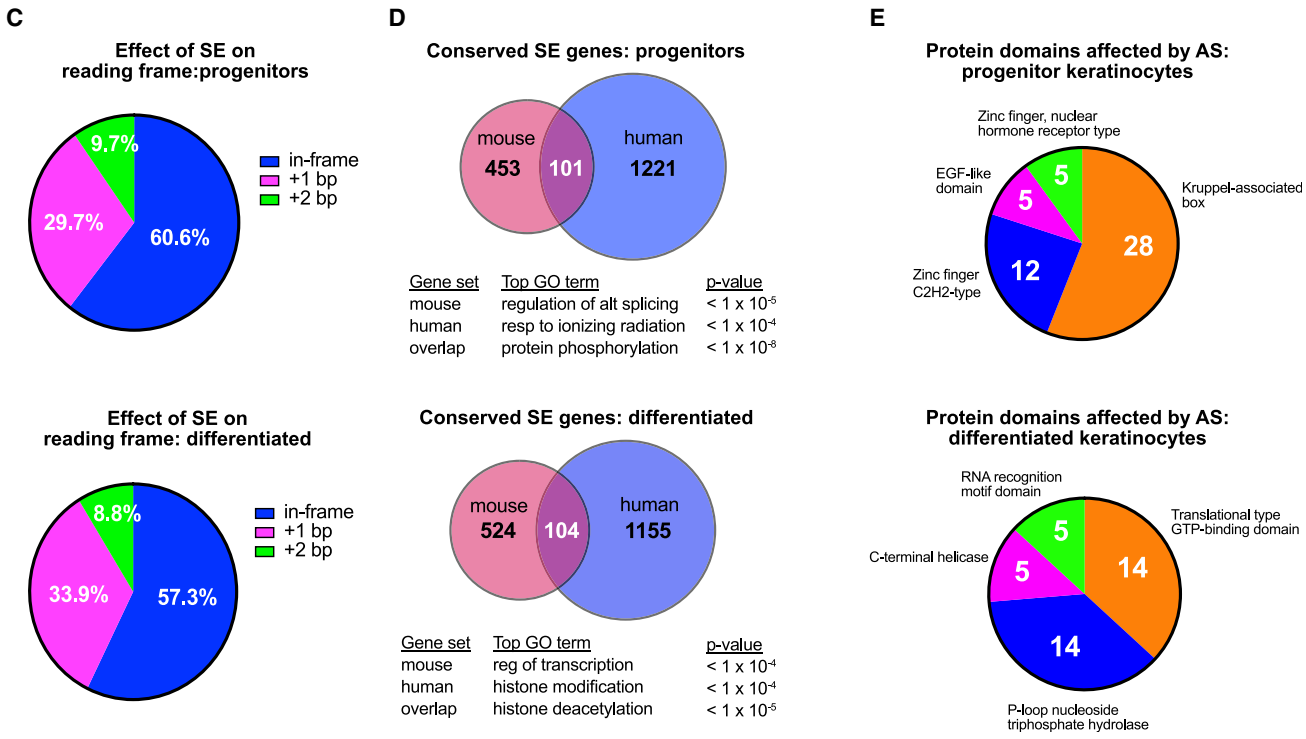

Figure 2. Characteristics of cassette exon AS events in epidermal keratinocytes

(A) Heatmap of cassette exon AS events. Identities of representative key epidermal regulator genes are noted.

(B) Ontology analysis of genes alternatively spliced between progenitor and differentiated keratinocytes.

(C) Proportion of spliced exon events predicted to cause in-frame insertion or frameshift.

(D) Overlap of alternatively spliced genes in mouse and human epidermal keratinocytes. The most highly enriched Gene Ontology (GO) term associated with shared vs. organism-specific mouse/human SE genes is shown.

(E) Impact of keratinocyte SE events on protein domains. Protein domains affected by 5 or more distinct AS events are shown.

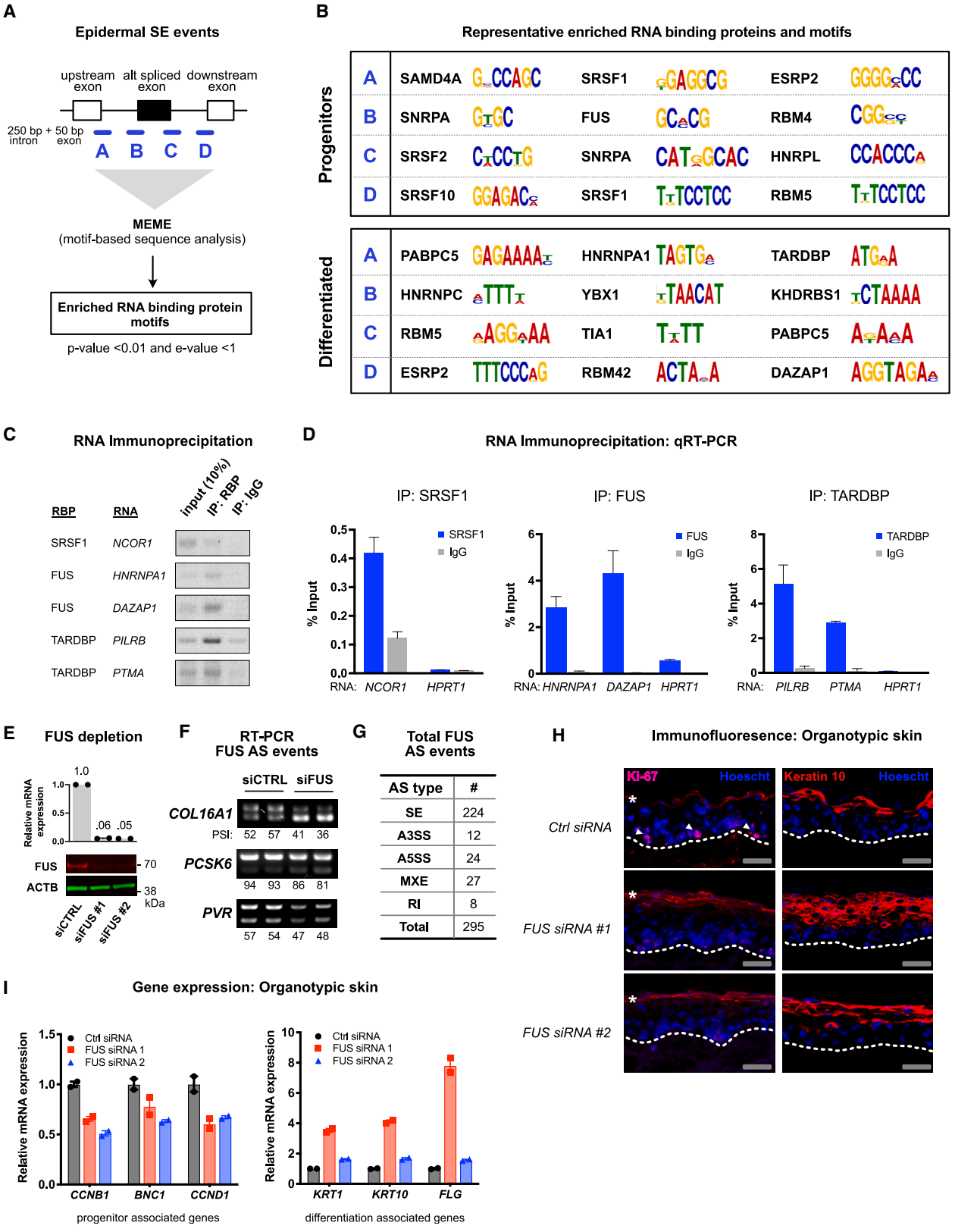

(legend on next page)

An SRSF1:*NCOR1* interaction served as a positive experimental control. Each RBP:RNA interaction displayed specificity by nature of its enrichment over a matched immunoglobulin G antibody control and a non-interaction control mRNA transcript, *HPRT1* (Figure 3D).

Having found that this strategy could identify binding of predicted epidermal RBP candidates to target mRNAs, we further evaluated this result by testing the potential epidermal function of FUS, which has been described in the epidermis[31] but whose function has not been thoroughly tested. We performed RNAi-mediated depletion of FUS using two independent short interfering RNAs (siRNAs) in primary human epidermal keratinocytes (Figure 3E), followed by RNA-seq and AS analysis. Depletion of FUS resulted in changes to 295 AS events, based on a threshold of $|\Delta PSI| > 0.1$ and FDR <0.05. Altered cassette exon splicing to representative AS events in COL16A1, PCSK6, and PVR were verified by RT-PCR (Figure 3F). Overall, SE events were the predominant type of AS event occurring with FUS depletion, accounting for over 75% of splicing changes (Figure 3G).

We next assessed epidermal stratification, proliferation, and differentiation of FUS-depleted human epidermal organotypic tissues (Figure 3H). In control tissue, immunofluorescence staining of Ki-67 marks proliferating keratinocytes of the basal layer. In two independent FUS siRNA knockdown tissues, we observed reduced Ki-67 staining compared to control, indicating a reduction of basal layer proliferation. To evaluate tissue differentiation, we also performed immunofluorescence for keratin 10, a protein expressed in suprabasal layers of the epidermis, focusing on an early differentiation time point of organotypic tissue. Compared to control tissue, in FUS-depleted tissue, we observed increased intensity of keratin 10 that extended to lower keratinocyte strata. To complement the results of tissue immunofluorescence, we quantitated transcript markers of proliferation and differentiation (Figure 3I). The proliferation-associated transcripts *CCNB1*, *CCND1*, and *BNC1* were reduced upon FUS depletion compared to control, whereas the differentiation markers *KRT1*, *KRT10*, and *FLG* were increased. These results suggested that FUS is an RBP that promotes epidermal keratinocyte proliferation and inhibits differentiation.

In summary, we combined information from epidermal gene expression, AS, *cis*-regulatory sequence motifs, and RNA-protein interaction data to identify a set of RBP candidates that regulate SE alternative mRNA splicing in the epidermis. We demonstrate an investigative pathway to use this information to identify and study functional RBPs in the skin.

AS of *MAP3K7* regulates the switch to epidermal differentiation

Finally, we pivoted from examining RBPs to look at epidermal AS events. We decided to focus on an AS event in mitogen-activated protein kinase kinase kinase 7 (*MAP3K7*), which encodes the transforming growth factor-β-activated kinase 1 (TAK1) protein. We selected this specific AS event for several reasons: first, *MAP3K7* has an established role in epidermal development.[45] Second, the AS event identified in *MAP3K7*, which involves differential inclusion of an 81-bp exon 12, is known to have important biological effects in other tissues and organisms: in murine development, loss of the shorter *MAP3K7* isoform is linked to defective proliferation of neural crest cells and formation of cleft palate.[46] In epithelial cancer cell lines, the short isoform promotes epithelial-mesenchymal transition, while the long isoform promotes apoptosis.[47] In humans, different mutations to *MAP3K7* result in phenotypically distinct conditions,[48] reflecting a complexity of *MAP3K7* genotype-phenotype correlations and its pleiotropic impact. Finally, the overall steady-state mRNA expression of *MAP3K7* does not change significantly during epidermal differentiation. Therefore, we reasoned that *MAP3K7* function in the epidermis may not be principally regulated by changes to overall expression but rather to mechanisms such as AS.

MAP3K7 is expressed in two mRNA isoforms in the epidermis (Figure 4A). The isoform that excludes exon 12 will be referred as *MAP3K7-short* and the isoform that includes exon 12 as *MAP3K7-long*. *MAP3K7-short* is preferentially expressed in keratinocyte progenitors *in vitro* (Figure 4A) and *in vivo* (Figure 1C). Upon differentiation, keratinocytes switch to preferential expression of *MAP3K7-long*. We verified the isoform switch in primary keratinocytes *in vitro* using RT-PCR, as well as in basal/progenitor and suprabasal/differentiated layers of adult human skin isolated by laser capture microdissection (Figure 4B). All biological replicates of *in vitro* and *in vivo* data (both flow-sorted keratinocytes in Figure 1C and laser-captured epidermal layers in Figure 4B) showed consistent patterns of enriched *MAP3K7-short* expression in basal/progenitors and *MAP3K7-long* in suprabasal/differentiated keratinocytes.

To evaluate if each *MAP3K7* isoform had a distinct role in keratinocyte differentiation, we designed isoform-specific RNA interference to preferentially deplete each *MAP3K7* isoform. To target the *MAP3K7-short* isoform, we used siRNA spanning the exon 11-to-13 junction. For *MAP3K7-long*, we used an siRNA targeting exon 12 (Figures 4B and 4C). RT-PCR using primers

Figure 3. RNA-binding proteins (RBPs) participating in epidermal AS cassette exon events

(A) Scheme of sequence motif analysis of AS exons in epidermal differentiation.

(B) Representative RBPs and their binding motifs enriched at each cassette exon splicing junction. A–D lettering corresponds to the exon-intron junctions shown in (A). The complete list of predicted RBPs and their binding motifs are in Table S2.

(C) RNA immunoprecipitation of candidate RBPs and their predicted RNA targets. SRSF1 is a positive control.

(D) Quantitative RT-PCR of RNA immunoprecipitation. *HPRT* is a negative/specificity control RNA. Data are means ± SEM (n = 3).

(E) Quantitative RT-PCR and immunoblot of FUS after treatment of keratinocytes with control (siCTRL) or FUS-targeting siRNAs (siFUS).

(F) RT-PCR of alternatively spliced SE events associated with FUS depletion.

(G) Number and type of alternative mRNA splicing events associated with FUS depletion.

(H) Immunofluorescence of control and FUS-depleted epidermal organotypic tissues. Ki-67 marks proliferating keratinocytes (pink, arrowheads); KRT10 is a differentiation-associated protein (orange/red). White asterisks indicate non-specific antibody staining of cornified layer. Scale bars (gray): 50 μm.

(I) Quantitative RT-PCR of progenitor-associated (*CCNB1*, *BNC1*, *CCND1*) and differentiation-associated (*KRT1*, *KRT10*, *FLG*) transcripts in epidermal organotypic tissue. Data are means ± SEM (n = 2).

Table 1. Candidate RBPs mediating cassette exon alternative splicing in epidermal differentiation

RNA-binding protein	Epidermal expression (Human Protein Atlas)	Role in epidermis (reference)
ANKHD1	high	none found
CNOT4	high	none found
CPEB4	N/A	none found
DAZAP1	high	none found
ESRP2	high	14
FUS	high	31
G3BP2	medium	none found
HNRNPA1	high	32
HNRNPA2B1	high	33
HNRNPC	high	none found
HNRNPH2	high	34
HNRNPLL	high	34
HuR/ELAVL1	medium	35
KHDRBS1	high	36
PABPC1	medium	none found
PABPC5	medium	none found
PABPN1	medium	37
PTBP1	high	38
RALY	high	none found
RBM4	medium	none found
RBM42	high	none found
RBM5	high	none found
RBM6	high	none found
SAMD4A	medium	none found
SART3	high	39
SNRPA	high	none found
SRSF1	high	29
SRSF10	high	40
SRSF2	high	41
TARDBP	high	none found
TIA1	N/A	none found
U2AF2	medium	none found
YBX1	medium	30
ZC3H14	medium	none found

specific to each isoform demonstrated preferential depletion of the targeted isoform (Figure 4C), although the *MAP3K7-short* siRNA showed partial knockdown of the long isoform, likely due to sequence overlap.

The protein product of *MAP3K7*, TAK1, regulates nuclear factor κB (NF-κB) signaling in the skin,[45] although it is not known if its two isoforms have distinct effects on NF-κB activity. To test this possibility, we measured NF-κB activity in primary human keratinocytes after RNAi depletion of the short vs. long isoforms (Figure 4D). We performed immunoblotting of a marker of canonical NF-κB activity, phosphorylated p65/RelA (p-p65), as well as proteins upstream (phosphorylated IKKa/b) and downstream (CCND1 and CCNE1) in the pathway. We also treated keratinocytes with tumor necrosis factor α to stimulate NF-κB pathway activation. We observed distinct effects from depletion of each MAP3K7 isoform: knockdown of *MAP3K7-long* had no effect on p-p65, whereas knockdown of *MAP3K7-short* led to reduced p-p65 (Figures 4D and 4E). The same pattern was noted for the downstream transcriptional targets CCND1 and CCNE1. By contrast, phosphorylated IKKa/b was inhibited by knockdown of either *MAP3K7* isoform. Because the isoform-targeting siRNAs were not fully specific, we also performed overexpression of the short and long isoforms (Figure 4F) to further assess for distinct activity of each isoform. Using an ELISA that measured phosphorylated p65/RelA, we found that short isoform overexpression increased p-p65, whereas long isoform expression did not (Figure 4G). Together, the results of these experiments indicate that the short and long *MAP3K7*/TAK1 isoforms have distinct effects on NF-κB signaling in keratinocytes.

The NF-κB pathway has a vital but complex relationship with epidermal homeostasis, inflammation, and carcinogenesis.[49–51] The pathway is hyperactivated throughout the epidermis in individuals with psoriasis, a condition characterized by excessive thickening and proliferation of keratinocytes.[52] To assess the impact of *MAP3K7* isoforms on epidermal differentiation, we evaluated the phenotype of *MAP3K7* isoform-targeted depletion in human epidermal organotypic tissue. To further test if inhibition of NF-κB signaling was involved in the tissue phenotype, we also generated organoids that were treated with protein kinase C (PKC), an NF-κB pathway activator, to assess if this treatment would rescue the *MAP3K7* knockdown phenotype. First, we confirmed that *MAP3K7* isoform depletion inhibited NF-κB activity in regenerated epidermal organoids by immunoblot of p-p65 (Figure 5A). We also found that treatment with 1 μM PKC prior to endpoint analysis was able to partially restore the depletion of p-p65 (Figure 5A).

Next, we evaluated the epidermal tissues by immunofluorescence staining of Ki-67 as a measure of cell proliferation (Figure 5B). As expected, control tissues showed Ki-67+ cells decorating a subset of cells along the basal layer. Depletion of the *MAP3K7-short* isoform resulted in a moderate reduction of Ki-67+ cells (Figures 5B and 5C). The most notable phenotype arose from depletion of the *MAP3K7-long* isoform, which resulted in increased Ki-67+ staining and labeling of keratinocytes in higher layers of the stratified tissue. In normal epidermis and organotypic tissue, Ki-67+ cells are confined to the innermost basal layer. The suprabasal expression indicated ectopic proliferation of suprabasal keratinocytes in *MAP3K7-long*-depleted epidermis and suggested that the demarcation between progenitor and differentiated keratinocytes was disrupted.

We also performed immunofluorescence staining for keratin 10, an epidermal protein that functions to provide mechanical strength and structure to the skin and is expressed in the differentiated layers of the epidermis (Figure 5B). Depletion of *MAP3K7-long* showed strongly reduced keratin 10 expression, indicating impaired differentiation. By contrast, *MAP3K7-short* depletion showed amplified intensity and increased distribution of keratin 10, reflecting accelerated epidermal differentiation (Figures 5B and 5D). To test if the impact of *MAP3K7* isoforms on NF-κB signaling played a role in these

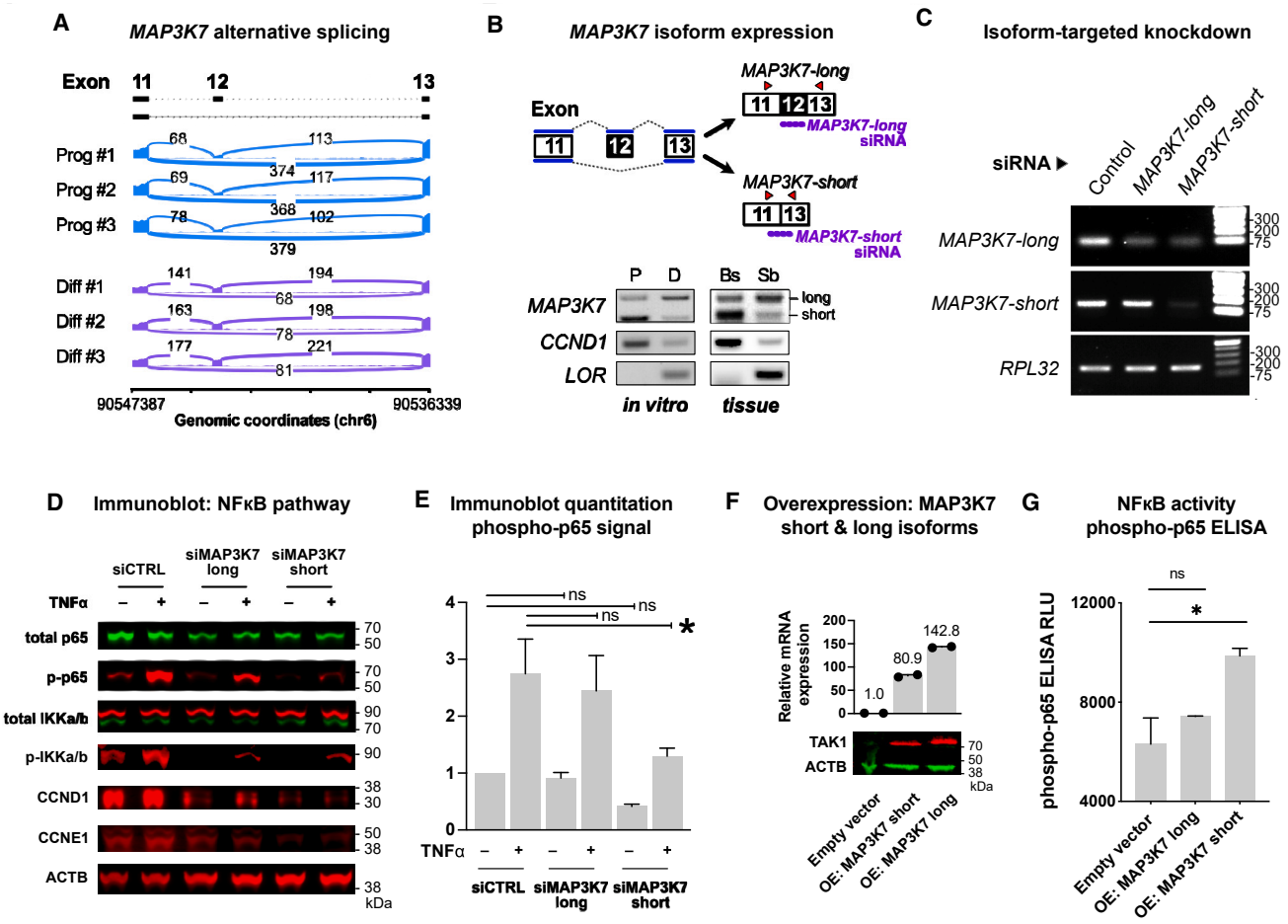

Figure 4. AS of *MAP3K7* exon 12 alters NF-κB activity in keratinocytes

(A) Sashimi plot showing enriched relative expression of exon-12-containing isoforms of *MAP3K7* upon epidermal differentiation.

(B) Scheme of RT-PCR primers (red triangles) to discern *MAP3K7* isoforms containing (*MAP3K7-long*) or excluding exon 12 (*MAP3K7-short*). Purple bars represent isoform-targeting siRNAs for short and long *MAP3K7* transcripts. Bottom, RT-PCR of *in vitro* progenitor (P) and differentiated (D) keratinocytes and *in vivo* laser capture microdissected skin tissue of basal (Bs) progenitor and suprabasal (Sb) differentiated layers. *CCND1* and *LOR* are control transcripts enriched in progenitor and differentiated states, respectively.

(C) RT-PCR evaluating *MAP3K7* isoform expression after transfection of isoform-targeting siRNAs against short and long isoforms. *RPL32* is an invariant expression control.

(D) Immunoblot for proteins in the NF-κB signaling pathway in progenitor keratinocytes after treatment with control or *MAP3K7*-isoform-targeted siRNAs, in the presence or absence of tumor necrosis factor α (TNF-α; 10 ng/mL), to stimulate NF-κB signaling. TNF-α was applied for 30 min, and protein lysates were harvested 48 h later.

(E) Intensity quantitation of phospho-p65/RelA from immunoblot experiments. Phosphorylated p65 was normalized internally to total p65, and the unstimulated siCTRL signal was set to 1 for each biological replicate. Data are means ± SEM (n = 3) (one-way ANOVA with a Tukey's honestly significant difference [HSD] post hoc test), *p < 0.05.

(F) RT-PCR and immunoblot for TAK1, the protein product of *MAP3K7*, after overexpression (OE) of each isoform.

(G) ELISA for phosphorylated p65 in keratinocytes after OE of empty vector or *MAP3K7* short/long isoforms. Data are means ± SEM (n = 3) (one-way ANOVA with a Tukey's HSD post hoc test), *p < 0.05.

phenotypes, we compared the results of Ki-67 and keratin 10 staining 1 day after a 2-h treatment with PKC. The most notable effect was observed after treatment of *MAP3K7-short*-depleted tissues, which showed a recovery of Ki-67+ cell staining in the basal layer (Figure 5B). We appreciated a moderate effect on keratin 10 expression, with reduced overexpression of keratin 10 after PKC treatment in *MAP3K7-short*-depleted tissues.

Finally, we quantitated mRNA expression of a set of progenitor- and differentiation-associated genes from total mRNA harvested from organotypic tissues (Figures 5E and 5F). Using control siRNA as a benchmark, we found that knockdown of *MAP3K7-short* led to the reduction of progenitor-associated genes (*CCNB1*, *BNC1*, *CYR61*, *CCND1*) and to increased expression of differentiation genes (*KRT1*, *KRT10*, *LOR*, *LCE3D*, *FLG*). *MAP3K7-long* knockdown had the opposite

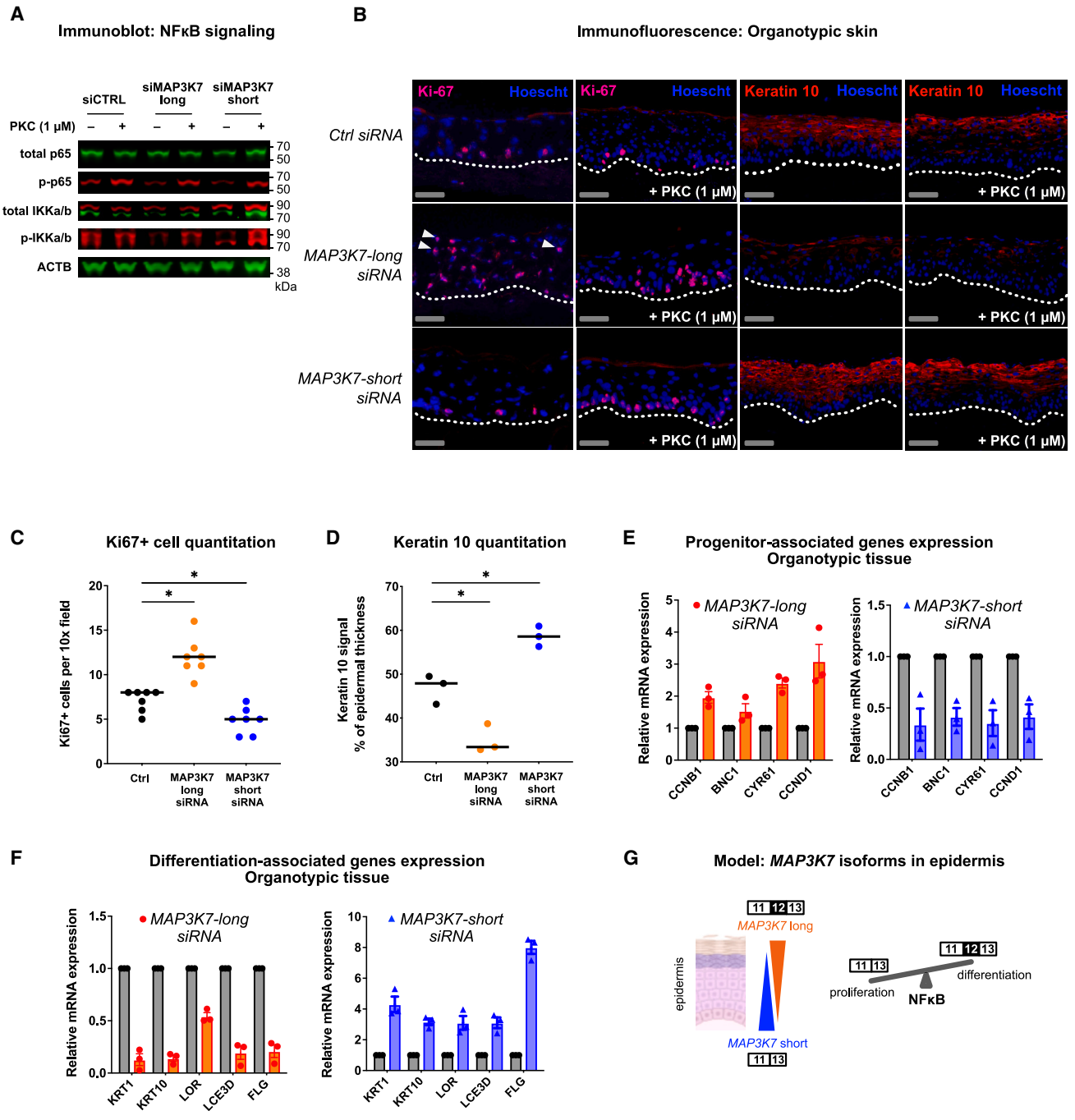

Figure 5. AS of *MAP3K7* exon 12 regulates epidermal differentiation

(A) Immunoblot for proteins in the NF-κB signaling pathway after treatment with control or *MAP3K7*-isoform-targeted siRNAs, in the presence of absence of protein kinase C (PKC), to stimulate NF-κB signaling.

(B) Immunofluorescence of Ki-67 and KRT10 in epidermal organotypic tissues generated with CTRL, *MAP3K7-long*, or *MAP3K7-short* siRNA-treated primary epidermal keratinocytes. Dotted white lines denote the basement membrane. Arrowheads highlight examples of proliferating keratinocytes detected in suprabasal layers. PKC treatment was applied for 2 h on the day prior to endpoint to evaluate the effect of NF-κB activation on the tissue phenotype. Scale bars (gray): 50 μm.

(C and D) Quantitation of (C) Ki-67+ cells and (D) KRT10 signal in epidermal organotypic tissues generated with CTRL, *MAP3K7-long*, or *MAP3K7-short* siRNAs. Data are means ± SEM (one-way ANOVA with a Tukey's HSD post hoc test) *p < 0.05.

(legend continued on next page)

effect: progenitor-associated gene expression was elevated, while differentiation-associated gene expression was repressed.

Viewed together, the tissue phenotype and gene expression profiles of human organotypic epidermis indicated that *MAP3K7-short* expression is enriched in basal progenitors and actively functions to promote the undifferentiated state. Upon differentiation, epidermal keratinocytes transition to preferential expression of *MAP3K7-long*, which promotes induction of keratinocyte differentiation. At least in part, these phenotypes appear to arise from distinct effects of *MAP3K7*/TAK1 isoforms on NF-κB signaling. These findings revealed that the AS of an 81-bp exon of a single gene is sufficient to influence the spatial and temporal dynamics of epidermal differentiation (Figure 5G).

DISCUSSION

Alternative mRNA splicing is a biological mechanism that diversifies the functions of RNAs and proteins and has integral roles in human development[7] and disease.[53] While public databases contain detailed information about transcript and protein expression in different tissues, biological states, and developmental time points, it can be challenging to find accessible, high-depth data on isoform-specific expression. However, the broad impact of AS on tissue functions argues for the importance of assessing the dynamic isoform changes in cell types and cell states within a tissue.

In this study, we found that thousands of AS events characterize the progenitor and differentiated state of epidermal keratinocytes, demonstrating extensive AS associated with the establishment and maintenance of epidermal homeostasis. A recent report demonstrated that changes in glucose supply to keratinocytes disrupts epidermal homeostasis by affecting the splicing of genes that control epidermal differentiation,[54] highlighting the importance of AS as a functional mediator that links metabolism and skin function. In our dataset, we noted that hundreds of epidermal genes showed substantial shifts in isoform expression in the absence of changes to overall steady-state mRNA expression. It is common for gene expression to be interpreted as a signal of gene activity. However, the results shown here and the specific example of *MAP3K7* indicate that functional isoform changes occur in the absence of major changes to overall expression.

At the same time, the opposite scenario is also true: AS itself can serve as a mechanism to regulate mRNA expression. We observed that ~40% of epidermal SE events cause a frameshift, which can trigger nonsense-mediated decay and transcript degradation.[55] A related mechanism may be indicated by the disproportionate number of RI events in progenitor keratinocytes compared to differentiated keratinocytes (Figure 1B). Transcripts with RIs can have several fates; one consequence is faster degradation of transcripts with RIs.[56] Intron retention was recently found to have a direct role in epidermal homeostasis by controlling expression of transcription factors that activate differentiation genes.[54] Consistent with these recent findings, when we examine the mRNA levels of epidermal AS genes with RIs compared to those without, we observe a decreased steady-state expression of RI genes in progenitor keratinocytes (Figure S2). These findings suggest that intron retention may have a broad impact on post-transcriptional regulation and transcript stability in the epidermis. Other types of splicing events are likely to have distinct post-transcriptional effects as well.

To explore the potential role of unstudied AS events in the epidermis, we characterized the role of different mRNA isoforms of *MAP3K7* in keratinocyte differentiation. We observed higher expression of the short *MAP3K7* mRNA isoform in epidermal progenitors and of the long isoform in differentiated cells. Using isoform-specific RNAi depletion, we demonstrated that the spatial expression of each isoform is not simply correlative but has an active role in promoting the progenitor or differentiated state. The protein product of *MAP3K7*, TAK1, is a kinase and key regulator of signaling. *MAP3K7* is representative of other alternatively spliced genes in this dataset that disproportionately involve regulators of phosphorylation, histone modification, signal transduction, organelle assembly, and even RNA splicing itself (Figure 6). In our supplemental information, we provide a list of epidermal AS events and genes that affect genes involved with keratinocyte cell-fate decisions (Table S3) as well as a list of epidermal genes and AS events in our dataset that overlap with AS events in psoriasis RNA-seq data (Table S4). We believe that these AS events are valuable candidates to test for potential roles in normal skin development and disease. Ultimately, these insights may provide new splicing-related biological targets for disease therapy.[4,53]

We speculate that a significant number of epidermal AS events in this study will have a functional role in epidermal processes and that they are not simply the result of a bystander effect of differentiation or the result of transcriptional splicing noise. To our knowledge, most of the epidermal AS events identified here have not been experimentally tested for function. However, the extensive number of AS events in the skin underscore the potential significance of AS in the maintenance of a constantly self-renewing somatic epithelium.

Limitations of the study

Our sequencing approach used 150-bp paired-end reads to detect and quantitate splicing events, but the read length was not long enough to phase multiple AS events on the same transcript. We considered using long-read sequencing technologies but chose to leverage the benefits of greater sequencing depth, less sequencing bias and error rates,[57] and more developed splicing analysis algorithms that were available with our chosen approach. Another limitation is that our principal dataset was generated from primary human keratinocytes differentiated *in vitro*, an experimental cell culture model that recapitulates most of the transcriptome of human skin tissue[58] but shows

(E) Quantitative RT-PCR of progenitor-associated genes in epidermal organotypic tissues. Relative expression of each gene is shown for each isoform-specific knockdown relative to its expression in control (gray bars, normalized to 1.0). Data are means ± SEM (n = 3).

(F) Quantitative RT-PCR of differentiation-associated genes in epidermal organotypic tissues. Data are means ± SEM (n = 3).

(G) Working model of *MAP3K7* isoform spatial expression within the epidermis and proposed effects of each isoform on NF-κB signaling and epidermal differentiation.

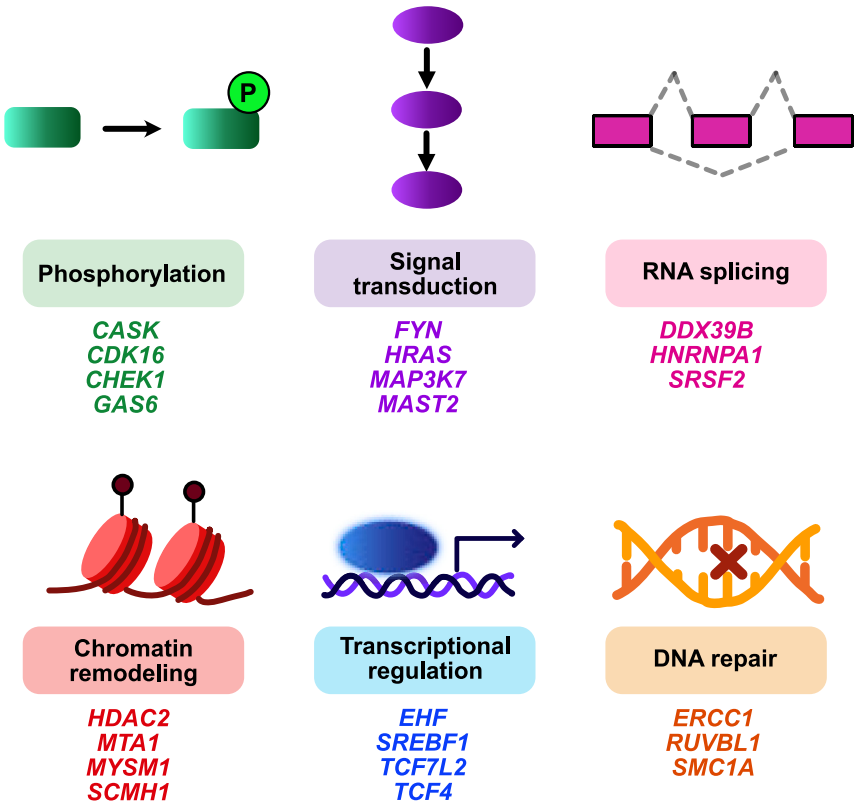

Figure 6. Highlights of alternatively spliced genes and processes involved in epidermal homeostasis

Schematic of major biological processes and representative alternatively spliced genes in human epidermis.

variability depending on the growth conditions and choice of differentiation stimulus.[15,59]

Laser-capture microdissected[54] epidermis did not yield the quantity and quality of RNA sufficient for reliable sequencing quality, depth, and transcript diversity for robust mRNA isoform analysis, especially for transcripts expressed at lower levels. We also performed flow sorting for ITGB4+ cells (Figure 1C) to enrich progenitor keratinocytes from epidermal tissue. Although expression of differentiation genes indicated that ITGB4-high and -low fractions did partition keratinocytes by differentiation status, the isolated ITGB4-high cells comprised only <1% of total keratinocytes (Figure S1E), much less than the expected progenitor fraction. This suggests a technical limitation in robustly separating viable progenitors with this approach. Using these alternative *in vivo* assessments to compare with *in vitro* splicing events, we found that many AS events and isoform expression patterns were concordant between *in-vitro*-cultured keratinocytes and *in vivo* epidermal RNA tissue but that some isoform expression patterns did not concur. Therefore, we recommend that any splicing events chosen for study from this dataset be first confirmed *in vivo*.

An additional experimental limitation is that we were unable to generate multiple independent siRNA sequences to perform *MAP3K7* isoform-specific knockdown due to the limited sequence that was unique to each isoform. Additionally, isoform-specific antibodies were not available to discern protein expression of each isoform. Finally, we note that the candidate set of RBPs associated with epidermal SE events (Table 1) is likely to be incomplete. *Cis*-regulatory motif analysis can be a productive first approach to identify candidate RBPs,[55] but mRNA splicing involves contribution of complex *cis*- and *trans*-factors[60] that cannot be fully captured by local sequence analysis.[43]

STAR★METHODS

Detailed methods are provided in the online version of this paper and include the following:

- KEY RESOURCES TABLE
- RESOURCE AVAILABILITY
  - Lead contact
  - Materials availability
  - Data and code availability
- EXPERIMENTAL MODEL AND SUBJECT DETAILS
  - Primary human epidermal keratinocytes
  - Organotypic culture
- METHOD DETAILS
  - RNA isolation, RT-PCR and qRT-PCR
  - RNA sequencing
  - Alternative splicing events analysis
  - Flow sort experiment
  - RNA immunoprecipitation
  - Protein isolation and immunoblot
  - siRNA transfection
  - MAP3K7 long and short isoform overexpression
  - NF-κB ELISA

SUPPLEMENTAL INFORMATION

Supplemental information can be found online at https://doi.org/10.1016/j.celrep.2024.113814.

ACKNOWLEDGMENTS

B.K.S. is supported by the NIH grants K08AR067853 and DP2HG012441.

AUTHOR CONTRIBUTIONS

Conceptualization, S.T., A.B.C.O., K.Q., and B.K.S.; data curation, S.T., W.S., P.C., K.Q., and B.K.S.; formal analysis, S.T., W.S., S.I.P., P.C., Z.L., K.Q., and B.K.S.; investigation, S.T., A.B.C.O., S.I.P., J.B., M.M., O.A., B.C., E.T., R.J.O., and B.K.S.; software, W.S., P.C., Z.L., and K.Q.; supervision, K.Q. and B.K.S.; writing – original draft, A.B.C.O. and B.K.S.; writing – review & editing, S.T., W.S., A.B.C.O., K.Q., and B.K.S.

DECLARATION OF INTERESTS

The authors declare no competing interests.

Received: April 21, 2023
Revised: August 22, 2023
Accepted: February 1, 2024

REFERENCES

1. Pan, Q., Shai, O., Lee, L.J., Frey, B.J., and Blencowe, B.J. (2008). Deep surveying of alternative splicing complexity in the human transcriptome by high-throughput sequencing. Nat. Genet. *40*, 1413–1415. https://doi.org/10.1038/ng.259.
2. Pickrell, J.K., Pai, A.A., Gilad, Y., and Pritchard, J.K. (2010). Noisy Splicing Drives mRNA Isoform Diversity in Human Cells. PLoS Genet. *6*, e1001236. https://doi.org/10.1371/journal.pgen.1001236.
3. Tress, M.L., Abascal, F., and Valencia, A. (2017). Alternative Splicing May Not Be the Key to Proteome Complexity. Trends Biochem. Sci. *42*, 98–110. https://doi.org/10.1016/j.tibs.2016.08.008.
4. Mazin, P.V., Khaitovich, P., Cardoso-Moreira, M., and Kaessmann, H. (2021). Alternative splicing during mammalian organ development. Nat. Genet. *53*, 925–934. https://doi.org/10.1038/s41588-021-00851-w.
5. Zhang, X., Chen, M.H., Wu, X., Kodani, A., Fan, J., Doan, R., Ozawa, M., Ma, J., Yoshida, N., Reiter, J.F., et al. (2016). Cell-Type-Specific Alternative Splicing Governs Cell Fate in the Developing Cerebral Cortex. Cell *166*, 1147–1162.e15. https://doi.org/10.1016/j.cell.2016.07.025.
6. Llorian, M., Gooding, C., Bellora, N., Hallegger, M., Buckroyd, A., Wang, X., Rajgor, D., Kayikci, M., Feltham, J., Ule, J., et al. (2016). The alternative splicing program of differentiated smooth muscle cells involves concerted non-productive splicing of post-transcriptional regulators. Nucleic Acids Res. *44*, 8933–8950. https://doi.org/10.1093/nar/gkw560.
7. Baralle, F.E., and Giudice, J. (2017). Alternative splicing as a regulator of development and tissue identity. Nat. Rev. Mol. Cell Biol. *18*, 437–451. https://doi.org/10.1038/nrm.2017.27.
8. Wang, D., Eraslan, B., Wieland, T., Hallström, B., Hopf, T., Zolg, D.P., Zecha, J., Asplund, A., Li, L.H., Meng, C., et al. (2019). A deep proteome and transcriptome abundance atlas of 29 healthy human tissues. Mol. Syst. Biol. *15*, e8503. https://doi.org/10.15252/msb.20188503.
9. Kim, D.S., Risca, V.I., Reynolds, D.L., Chappell, J., Rubin, A.J., Jung, N., Donohue, L.K.H., Lopez-Pajares, V., Kathiria, A., Shi, M., et al. (2021). The dynamic, combinatorial cis-regulatory lexicon of epidermal differentiation. Nat. Genet. *53*, 1564–1576. https://doi.org/10.1038/s41588-021-00947-3.
10. Lopez-Pajares, V., Qu, K., Zhang, J., Webster, D.E., Barajas, B.C., Siprashvili, Z., Zarnegar, B.J., Boxer, L.D., Rios, E.J., Tao, S., et al. (2015). A LncRNA-MAF:MAFB Transcription Factor Network Regulates Epidermal Differentiation. Dev. Cell *32*, 693–706. https://doi.org/10.1016/j.devcel.2015.01.028.
11. Truong, A.B., Kretz, M., Ridky, T.W., Kimmel, R., and Khavari, P.A. (2006). p63 regulates proliferation and differentiation of developmentally mature keratinocytes. Genes Dev. *20*, 3185–3197. https://doi.org/10.1101/gad.1463206.
12. Leclerc, E.A., Huchenq, A., Kezic, S., Serre, G., and Jonca, N. (2014). Mice deficient for the epidermal Dermokine β and γ display transient cornification defects. J. Cell Sci., 2862–2872. https://doi.org/10.1242/jcs.144808.
13. Smits, P., Poumay, Y., Karperien, M., Tylzanowski, P., Wauters, J., Huylebroeck, D., Ponec, M., and Merregaert, J. (2000). Differentiation-Dependent Alternative Splicing and Expression of the Extracellular Matrix Protein 1 Gene in Human Keratinocytes. J. Invest. Dermatol. *114*, 718–724. https://doi.org/10.1046/j.1523-1747.2000.00916.x.
14. Bebee, T.W., Park, J.W., Sheridan, K.I., Warzecha, C.C., Cieply, B.W., Rohacek, A.M., Xing, Y., and Carstens, R.P. (2015). The splicing regulators Esrp1 and Esrp2 direct an epithelial splicing program essential for mammalian development. Elife *4*, e08954. https://doi.org/10.7554/eLife.08954.
15. Tanis, S.E.J., Jansen, P.W.T.C., Zhou, H., van Heeringen, S.J., Vermeulen, M., Kretz, M., and Mulder, K.W. (2018). Splicing and Chromatin Factors Jointly Regulate Epidermal Differentiation. Cell Rep. *25*, 1292–1303.e5. https://doi.org/10.1016/j.celrep.2018.10.017.
16. Shen, S., Park, J.W., Lu, Z.x., Lin, L., Henry, M.D., Wu, Y.N., Zhou, Q., and Xing, Y. (2014). rMATS: Robust and flexible detection of differential alternative splicing from replicate RNA-Seq data. Proc. Natl. Acad. Sci. USA *111*, E5593–E5601. https://doi.org/10.1073/pnas.1419161111.
17. Lev-Maor, G., Goren, A., Sela, N., Kim, E., Keren, H., Doron-Faigenboim, A., Leibman-Barak, S., Pupko, T., and Ast, G. (2007). The "Alternative" Choice of Constitutive Exons throughout Evolution. PLoS Genet. *3*, e203. https://doi.org/10.1371/journal.pgen.0030203.
18. Wu, N., Rollin, J., Masse, I., Lamartine, J., and Gidrol, X. (2012). p63 Regulates Human Keratinocyte Proliferation via MYC-regulated Gene Network and Differentiation Commitment through Cell Adhesion-related Gene Network. J. Biol. Chem. *287*, 5627–5638. https://doi.org/10.1074/jbc.M111.328120.
19. Sun, B.K., Boxer, L.D., Ransohoff, J.D., Siprashvili, Z., Qu, K., Lopez-Pajares, V., Hollmig, S.T., and Khavari, P.A. (2015). CALML5 is a ZNF750- and TINCR-induced protein that binds stratifin to regulate epidermal differentiation. Genes Dev. *29*, 2225–2230. https://doi.org/10.1101/gad.267708.115.
20. Perez-Moreno, M., Davis, M.A., Wong, E., Pasolli, H.A., Reynolds, A.B., and Fuchs, E. (2006). p120-Catenin Mediates Inflammatory Responses in the Skin. Cell *124*, 631–644. https://doi.org/10.1016/j.cell.2005.11.043.
21. Nanba, D., Toki, F., Matsushita, N., Matsushita, S., Higashiyama, S., and Barrandon, Y. (2013). Actin filament dynamics impacts keratinocyte stem cell maintenance. EMBO Mol. Med. *5*, 640–653. https://doi.org/10.1002/emmm.201201839.
22. Conte, M.I., Pescatore, A., Paciolla, M., Esposito, E., Miano, M.G., Lioi, M.B., McAleer, M.A., Giardino, G., Pignata, C., Irvine, A.D., et al. (2014). Insight into IKBKG/NEMO Locus: Report of New Mutations and Complex Genomic Rearrangements Leading to Incontinentia Pigmenti Disease. Hum. Mutat. *35*, 165–177. https://doi.org/10.1002/humu.22483.
23. Damen, M., Wirtz, L., Soroka, E., Khatif, H., Kukat, C., Simons, B.D., and Bazzi, H. (2021). High proliferation and delamination during skin epidermal

stratification. Nat. Commun. *12*, 3227. https://doi.org/10.1038/s41467-021-23386-4.

24. Barbosa-Morais, N.L., Irimia, M., Pan, Q., Xiong, H.Y., Gueroussov, S., Lee, L.J., Slobodeniuc, V., Kutter, C., Watt, S., Çolak, R., et al. (2012). The Evolutionary Landscape of Alternative Splicing in Vertebrate Species. Science *338*, 1587–1593. https://doi.org/10.1126/science.1230612.

25. Papasaikas, P., and Valcárcel, J. (2012). Splicing in 4D. Science *338*, 1547–1548. https://doi.org/10.1126/science.1233219.

26. Merkin, J., Russell, C., Chen, P., and Burge, C.B. (2012). Evolutionary Dynamics of Gene and Isoform Regulation in Mammalian Tissues. Science *338*, 1593–1599. https://doi.org/10.1126/science.1228186.

27. Blum, M., Chang, H.-Y., Chuguransky, S., Grego, T., Kandasaamy, S., Mitchell, A., Nuka, G., Paysan-Lafosse, T., Qureshi, M., Raj, S., et al. (2021). The InterPro protein families and domains database: 20 years on. Nucleic Acids Res. *49*, D344–D354. https://doi.org/10.1093/nar/gkaa977.

28. Bailey, T.L., Boden, M., Buske, F.A., Frith, M., Grant, C.E., Clementi, L., Ren, J., Li, W.W., and Noble, W.S. (2009). MEME SUITE: tools for motif discovery and searching. Nucleic Acids Res. *37*, W202–W208. https://doi.org/10.1093/nar/gkp335.

29. Yu, T., Cazares, O., Tang, A.D., Kim, H.-Y., Wald, T., Verma, A., Liu, Q., Barcellos-Hoff, M.H., Floor, S.N., Jung, H.-S., et al. (2022). SRSF1 governs progenitor-specific alternative splicing to maintain adult epithelial tissue homeostasis and renewal. Dev. Cell *57*, 624–637.e4. https://doi.org/10.1016/j.devcel.2022.01.011.

30. Kwon, E., Todorova, K., Wang, J., Horos, R., Lee, K.K., Neel, V.A., Negri, G.L., Sorensen, P.H., Lee, S.W., Hentze, M.W., and Mandinova, A. (2018). The RNA-binding protein YBX1 regulates epidermal progenitors at a post-transcriptional level. Nat. Commun. *9*, 1734. https://doi.org/10.1038/s41467-018-04092-0.

31. Chen, X., Lloyd, S.M., Kweon, J., Gamalong, G.M., and Bao, X. (2021). Epidermal progenitors suppress GRHL3-mediated differentiation through intronic polyadenylation promoted by CPSF-HNRNPA3 collaboration. Nat. Commun. *12*, 448. https://doi.org/10.1038/s41467-020-20674-3.

32. Cheunim, T., Zhang, J., Milligan, S.G., McPhillips, M.G., and Graham, S.V. (2008). The alternative splicing factor hnRNP A1 is up-regulated during virus-infected epithelial cell differentiation and binds the human papillomavirus type 16 late regulatory element. Virus Res. *131*, 189–198. https://doi.org/10.1016/j.virusres.2007.09.006.

33. Zhou, X., Brown, B.A., Siegel, A.P., El Masry, M.S., Zeng, X., Song, W., Das, A., Khandelwal, P., Clark, A., Singh, K., et al. (2020). Exosome-Mediated Crosstalk between Keratinocytes and Macrophages in Cutaneous Wound Healing. ACS Nano *14*, 12732–12748. https://doi.org/10.1021/acsnano.0c03064.

34. Li, J., Chen, Y., Tiwari, M., Bansal, V., and Sen, G.L. (2021). Regulation of integrin and extracellular matrix genes by HNRNPL is necessary for epidermal renewal. PLoS Biol. *19*, e3001378. https://doi.org/10.1371/journal.pbio.3001378.

35. Garcin, G., Guiraud, I., Lacroix, M., Genthon, C., Rialle, S., Joujoux, J.-M., Meunier, L., Lavabre-Bertrand, T., Stoebner, P.-E., and Le Gallic, L. (2015). AMPK/HuR-Driven IL-20 Post-Transcriptional Regulation in Psoriatic Skin. J. Invest. Dermatol. *135*, 2732–2741. https://doi.org/10.1038/jid.2015.282.

36. Fu, K., Sun, X., Xia, X., Hobbs, R.P., Guo, Y., Coulombe, P.A., and Wan, F. (2019). Sam68 is required for the growth and survival of nonmelanoma skin cancer. Cancer Med. *8*, 6106–6113. https://doi.org/10.1002/cam4.2513.

37. Mohibi, S., Zhang, J., and Chen, X. (2020). PABPN1, a Target of p63, Modulates Keratinocyte Differentiation through Regulation of p63α mRNA Translation. J. Invest. Dermatol. *140*, 2166–2177.e6. https://doi.org/10.1016/j.jid.2020.03.942.

38. Noiret, M., Mottier, S., Angrand, G., Gautier-Courteille, C., Lerivray, H., Viet, J., Paillard, L., Mereau, A., Hardy, S., and Audic, Y. (2016). Ptbp1 and Exosc9 knockdowns trigger skin stability defects through different pathways. Dev. Biol. *409*, 489–501. https://doi.org/10.1016/j.ydbio.2015.11.002.

39. Zhang, Z.H., Niu, Z.M., Yuan, W.T., Zhao, J.J., Jiang, F.X., Zhang, J., Chai, B., Cui, F., Chen, W., Lian, C.H., et al. (2005). A mutation in SART3 gene in a Chinese pedigree with disseminated superficial actinic porokeratosis. Br. J. Dermatol. *152*, 658–663. https://doi.org/10.1111/j.1365-2133.2005.06443.x.

40. He, R., Wu, S., Gao, R., Chen, J., Peng, Q., Hu, H., Zhu, L., Du, Y., Sun, W., Ma, X., et al. (2021). Identification of a Long Noncoding RNA TRAF3IP2-AS1 as Key Regulator of IL-17 Signaling through the SRSF10–IRF1–Act1 Axis in Autoimmune Diseases. J. Immunol. *206*, 2353–2365. https://doi.org/10.4049/jimmunol.2001223.

41. Sajini, A.A., Choudhury, N.R., Wagner, R.E., Bornelöv, S., Selmi, T., Spanos, C., Dietmann, S., Rappsilber, J., Michlewski, G., and Frye, M. (2019). Loss of 5-methylcytosine alters the biogenesis of vault-derived small RNAs to coordinate epidermal differentiation. Nat. Commun. *10*, 2550. https://doi.org/10.1038/s41467-019-10020-7.

42. Nasrin, F., Rahman, M.A., Masuda, A., Ohe, K., Takeda, J.I., and Ohno, K. (2014). HnRNP C, YB-1 and hnRNP L coordinately enhance skipping of human MUSK exon 10 to generate a Wnt-insensitive MuSK isoform. Sci. Rep. *4*, 6841. https://doi.org/10.1038/srep06841.

43. Chakrabarti, A.M., Haberman, N., Praznik, A., Luscombe, N.M., and Ule, J. (2018). Data Science Issues in Studying Protein–RNA Interactions with CLIP Technologies. Annu. Rev. Biomed. Data Sci. *1*, 235–261. https://doi.org/10.1146/annurev-biodatasci-080917-013525.

44. Van Nostrand, E.L., Freese, P., Pratt, G.A., Wang, X., Wei, X., Xiao, R., Blue, S.M., Chen, J.-Y., Cody, N.A.L., Dominguez, D., et al. (2020). A large-scale binding and functional map of human RNA-binding proteins. Nature *583*, 711–719. https://doi.org/10.1038/s41586-020-2077-3.

45. Omori, E., Matsumoto, K., Sanjo, H., Sato, S., Akira, S., Smart, R.C., and Ninomiya-Tsuji, J. (2006). TAK1 Is a Master Regulator of Epidermal Homeostasis Involving Skin Inflammation and Apoptosis. J. Biol. Chem. *281*, 19610–19617. https://doi.org/10.1074/jbc.M603384200.

46. Cibi, D.M., Mia, M.M., Guna Shekeran, S., Yun, L.S., Sandireddy, R., Gupta, P., Hota, M., Sun, L., Ghosh, S., and Singh, M.K. (2019). Neural crest-specific deletion of Rbfox2 in mice leads to craniofacial abnormalities including cleft palate. Elife *8*, e45418. https://doi.org/10.7554/eLife.45418.

47. Tripathi, V., Shin, J.-H., Stuelten, C.H., and Zhang, Y.E. (2019). TGF-β-induced alternative splicing of TAK1 promotes EMT and drug resistance. Oncogene *38*, 3185–3200. https://doi.org/10.1038/s41388-018-0655-8.

48. van Woerden, G.M., Senden, R., de Konink, C., Trezza, R.A., Baban, A., Bassetti, J.A., van Bever, Y., Bird, L.M., van Bon, B.W., Brooks, A.S., et al. (2022). The MAP3K7 gene: Further delineation of clinical characteristics and genotype/phenotype correlations. Hum. Mutat. *43*, 1377–1395. https://doi.org/10.1002/humu.24425.

49. Takao, J., Yudate, T., Das, A., Shikano, S., Bonkobara, M., Ariizumi, K., and Cruz, P.D. (2003). Expression of NF-kappaB in epidermis and the relationship between NF-kappaB activation and inhibition of keratinocyte growth. Br. J. Dermatol. *148*, 680–688. https://doi.org/10.1046/j.1365-2133.2003.05285.x.

50. Wullaert, A., Bonnet, M.C., and Pasparakis, M. (2011). NF-κB in the regulation of epithelial homeostasis and inflammation. Cell Res. *21*, 146–158. https://doi.org/10.1038/cr.2010.175.

51. Zhang, J.Y., Green, C.L., Tao, S., and Khavari, P.A. (2004). NF-κB RelA opposes epidermal proliferation driven by TNFR1 and JNK. Genes Dev. *18*, 17–22. https://doi.org/10.1101/gad.1160904.

52. Lizzul, P.F., Aphale, A., Malaviya, R., Sun, Y., Masud, S., Dombrovskiy, V., and Gottlieb, A.B. (2005). Differential Expression of Phosphorylated NF-κB/RelA in Normal and Psoriatic Epidermis and Downregulation of NF-κB in Response to Treatment with Etanercept. J. Invest. Dermatol. *124*, 1275–1283. https://doi.org/10.1111/j.0022-202X.2005.23735.x.

53. Urbanski, L.M., Leclair, N., and Anczuków, O. (2018). Alternative-splicing defects in cancer: Splicing regulators and their downstream targets, guiding the way to novel cancer therapeutics. WIREs RNA *9*, e1476. https://doi.org/10.1002/wrna.1476.

54. Miao, W., Porter, D.F., Lopez-Pajares, V., Siprashvili, Z., Meyers, R.M., Bai, Y., Nguyen, D.T., Ko, L.A., Zarnegar, B.J., Ferguson, I.D., et al. (2023). Glucose dissociates DDX21 dimers to regulate mRNA splicing and tissue differentiation. Cell *186*, 80–97.e26. https://doi.org/10.1016/j.cell.2022.12.004.

55. Lewis, B.P., Green, R.E., and Brenner, S.E. (2003). Evidence for the widespread coupling of alternative splicing and nonsense-mediated mRNA decay in humans. Proc. Natl. Acad. Sci. USA *100*, 189–192. https://doi.org/10.1073/pnas.0136770100.

56. Kumari, A., Sedehizadeh, S., Brook, J.D., Kozlowski, P., and Wojciechowska, M. (2022). Differential fates of introns in gene expression due to global alternative splicing. Hum. Genet. *141*, 31–47. https://doi.org/10.1007/s00439-021-02409-6.

57. Hu, Y., Fang, L., Chen, X., Zhong, J.F., Li, M., and Wang, K. (2021). LIQA: long-read isoform quantification and analysis. Genome Biol. *22*, 182. https://doi.org/10.1186/s13059-021-02399-8.

58. Gazel, A., Ramphal, P., Rosdy, M., De wever, B., Tornier, C., Hosein, N., Lee, B., Tomic-Canic, M., and Blumenberg, M. (2003). Transcriptional Profiling of Epidermal Keratinocytes: Comparison of Genes Expressed in Skin, Cultured Keratinocytes, and Reconstituted Epidermis, Using Large DNA Microarrays. J. Invest. Dermatol. *121*, 1459–1468. https://doi.org/10.1111/j.1523-1747.2003.12611.x.

59. Watt, F.M. (2016). Engineered Microenvironments to Direct Epidermal Stem Cell Behavior at Single-Cell Resolution. Dev. Cell *38*, 601–609. https://doi.org/10.1016/j.devcel.2016.08.010.

60. Marasco, L.E., and Kornblihtt, A.R. (2023). The physiology of alternative splicing. Nat. Rev. Mol. Cell Biol. *24*, 242–254. https://doi.org/10.1038/s41580-022-00545-z.

61. Li, J., and Sen, G.L. (2015). Generation of Genetically Modified Organotypic Skin Cultures Using Devitalized Human Dermis. J. Vis. Exp. *106*, e53280. https://doi.org/10.3791/53280.

STAR★METHODS

KEY RESOURCES TABLE

REAGENT or RESOURCE	SOURCE	IDENTIFIER
Antibodies		
TAK1 (D94D7) Rabbit mAb (1:1000)	Cell Signaling Technology	Cat #5206; RRID: AB_10694079
Phospho-TAK1 (Thr184/187) (90C7) Rabbit mAb (1:1000)	Cell Signaling Technology	Cat #4508; RRID: AB_561317
NF-kB p65 (L8F6) Mouse mAb (1:1000)	Cell Signaling Technology	Cat #6956; RRID: AB_10828935
Anti-Phospho-NF-kappaB p65 (Ser536) Rabbit Monoclonal Antibody (1:500)	Cell Signaling Technology	Cat #3033; RRID: AB_331284
NF-kB Pathway Antibody Sampler Kit p-p65, t-p65, t-IKKa, t-IKKb (1:1000) *p*-IKKa, pIKKb (1:500)	Cell Signaling Technology	Cat #9936
Cyclin D1 (E3P5S) XP Rabbit mAb	Cell Signaling Technology	Cat #55506; RRID: AB_2827374
Cyclin E1 (D7T3U) Rabbit mAb	Cell Signaling Technology	Cat #20808; RRID: AB_2783554
E7 anti-beta tubulin (1:1000)	Developmental Studies Hybridoma Bank	RRID: AB_2315513
IRDye 680RD anti-mouse (Donkey) (1:10000)	LI-COR Biosciences	Cat #926–68072; RRID: AB_10953628
IRDye 800CW anti-rabbit (Goat) (1:10000)	LI-COR Biosciences	Cat #926–32211; RRID: AB_621843
Cytokeratin 10 antibody	Abcam	Cat #ab76318; RRID: AB_1523465
Ki-67 Antibody	Invitrogen	Cat #MA5-14520; RRID: AB_10979488
Hoechst 33342	Cell signaling	Cat #4082; RRID: AB_10626776
Alexa Fluor 555 anti-rabbit antibody	Invitrogen	Cat #A21428; RRID: AB_2535849
Integrin B4 (A9)	Santa Cruz	Sc-13543
Chemicals, peptides, and recombinant proteins		
Epilife Medium, with 60uM calcium	Gibco	Cat #MEPI500CA
Human Keratinocyte Growth Supplement (HKGS)	Gibco	Cat #S0015
Antibiotic-Antimycotic (100x)	Gibco	Cat #1524096
0.25% Trypsin	Gibco	Cat #15050-065
DMEM	Gibco	Cat #11995
Ham's F12	Cambrex	Cat #12-615F
Penicillin-Streptomycin	Gibco	Cat #15140-122
FBS	Gibco	Cat #10437-028
adenine	Sigma	Cat #A-9795
hydrocortisone	Sigma	Cat #H0888
cholera toxin	Sigma	Cat #C-8052
transferrin	Sigma	Cat #T-0665
Triiodo-L-thyronine	Sigma	Cat #T-6397
EGF	Invitrogen	Cat #13247-051
Casein Blocking Buffer	Sigma-Aldrich	Cat #7594-1L
UltraPure 10% SDS	Invitrogen	Cat# 15553027
4X Bolt LDS Sample Buffer	Invitrogen	Cat# B0007
10X Bolt Sample Reducing Agent	Invitrogen	Cat# B0009
DreamTaq Green PCR Master Mix (2X)	Thermo Scientific	Cat# K1081
SYBR Safe DNA Gel Stain	Invitrogen	Cat# S33102
20X Bolt MOPS SDS Running Buffer	Invitrogen	Cat# B0001
Triton X-100	Nacalai tesque	Cat# 35501-15
RIPA Lysis Buffer	Millipore	Cat# 20-188

(*Continued on next page*)

Continued

REAGENT or RESOURCE	SOURCE	IDENTIFIER
Halt Protease and Phosphatase Inhibitor Cocktail	Thermo Scientific	Cat# 78440
Lipofectamine RNAiMAX Transfection Reagent	Invitrogen	Cat# 13778030
Attractene Transfection Reagent	Qiagen	Cat# 301005
Agarose	Fisher BioReagent	Cat# BP160-500
Human TNFa Recombinant Protein	Fisher Scientific	Cat# 210-TA-005
alamarBlue Cell Viability Reagent	Invitrogen	Cat# DAL1025
Tissue-Tek O.C.T. Compound	Sakura	Cat# 4583
Prostratin, PKC activator	abcam	Cat# ab120880
Critical commercial assays		
RNeasy Plus Mini Kit	Qiagen	Cat# 74136
iScript Reverse Transcription Supermix for RT-qPCR	Bio-Rad	Cat# 1708841
iTaq Universal SYBR Green Supermix	Bio-Rad	Cat# 1725124
Nuclear Extract Kit	Active Motif	Cat# 40010
TransAM NF-κB p65 Transcription Factor ELISA Kit	Active Motif	Cat# 40097
Deposited data		
RNA-seq data	This paper	GEO: GSE201094
Experimental models: Cell lines		
Human primary keratinocytes	This Paper	N/A
Experimental models: Organisms/strains		
Human Dermis	New York Firefighters Skin Bank	N/A
Oligonucleotides		
DsiRNA (MAP3K7 long) Forward	Integrated DNA Technologies	5′- CGUAAAACUGCUUCAUUUGGC AACA-3′
DsiRNA (MAP3K7 long) Reverse	Integrated DNA Technologies	5′- UGGCAUUUUGACGAAGUAAAC CGUUGU-3′
DsiRNA (MAP3K7 short) Forward	Integrated DNA Technologies	5′- CAAAGCAACAGAGUGAAUCUG GACGUU-3′
DsiRNA (MAP3K7 short) Reverse	Integrated DNA Technologies	5′- GUUUCGUUGUCUCACUUAGAC CUGCAA-3′
FUS siRNA-1	Thermo Fisher	S5401
FUS siRNA-2	Thermo Fisher	S533595
siRNA (negative control)	Thermo Fisher	Cat# 4390843
Primers for RT-PCR and qRT-PCR, see Table S6	This paper	N/A
Recombinant DNA		
pcDNA3.1-C-(k)DYK-MAP3K7 long	Genescript	Cat# OHu21832
pcDNA3.1-C-(k)DYK-MAP3K7 short	Genescript	Cat# OHu14588
Software and algorithms		
Prism 9	GraphPad software	www.graphpad.com
Image Lab Software (version: 4.0)	Bio-Rad	www.bio-rad.com
ImageJ (version: 10.0.7)	NIH	ImageJ.nih.gov/iJ/
Other		
SpectraMax iD3	Molecular Devices	N/A
EVOS M5000 Imaging System	Invitrogen	N/A
CFX Opus 384 Real-Time PCR System	Bio-Rad	www.bio-rad.com
T100 Thermal Cycler	Bio-Rad	www.bio-rad.com

RESOURCE AVAILABILITY

Lead contact

Further information and requests for resources and reagents should be directed to and will be fulfilled by the lead contact, Bryan Sun (sunb8@hs.uci.edu)

Materials availability

All unique/stable reagents generated in this study are available from the lead contact with a completed materials transfer agreement.

Data and code availability

- RNA sequencing data have been deposited at NIH Gene Expression Omnibus and are publicly available as of the date of publication. Accession number is listed in the key resources table. Microscopy data reported in this paper will be shared by the lead contact upon request.
- This paper does not report original code.
- Any additional information required to reanalyze the data reported in this paper is available from the lead contact upon request.

EXPERIMENTAL MODEL AND SUBJECT DETAILS

Primary human epidermal keratinocytes

Primary epidermal keratinocytes were isolated from discarded neonatal foreskin from circumcisions, collected upon written informed consent under an institutional review board protocol approved by the University of California, San Diego. Primary epidermal keratinocytes were propagated in EpiLife Medium (Thermo Fisher Scientific) with human keratinocyte growth supplement (HKGS; Cascade Biologics) and 1% antibiotic-antimycotic (Thermo Fisher Scientific), at 37°C and 5% CO_2. Differentiation was induced by plating cells to confluence and supplementing media with 1.2 mmol/L calcium.

Organotypic culture

Epidermal organotypic culture was performed essentially as described previously,[61] in which primary epidermal keratinocytes were seeded onto devitalized human dermis and cultured for stratification. To prepare devitalized human dermis, skin tissue was washed in 4× penicillin/streptomycin (pen/strep) in PBS. After shaking vigorously for 5 min, the skin tissue was transferred to a new tube with fresh 4× pen/strep/PBS. The skin tissue was kept in a tissue culture incubator at 37°C for 2 weeks to allow separation of the dermis from the epidermis. Under sterile conditions, the epidermis was peeled from the dermis. The dermis was washed in 4× pen/strep/PBS with vigorous shaking, transferred to a fresh 50 mL conical tube with pen/strep/PBS and stored at 4°C until use. Air-dried devitalized human dermis was mounted onto 1.7 cm × 1.7 cm supports, and 500,000 keratinocytes seeded onto the basement membrane size of the dermis. Epidermal keratinocytes were grown at the air-liquid interface over a course of 4 or 7 days, with media changed daily. Half of the final tissue was collected for RNA isolation, and the other half was embedded in O.C.T media (Sakura) and sectioned on a cryostat at 7μm thickness.

METHOD DETAILS

RNA isolation, RT-PCR and qRT-PCR

Total RNA was isolated with RNeasy Plus Mini Kit (QIAGEN). For human keratinocytes, 350 μL of RLT Plus buffer (QIAGEN) was added directly to cells prior to addition of 350μL of 70% EtOH and column-based isolation of RNA. For organotypic culture tissue, full thickness tissue was subjected to bead beating of 750μL of RNA lysis buffer. Tissue was then centrifuged, followed by adding of 350 μL of clarified lysate to 70% EtOH and column-based isolation of RNA. cDNA was reverse transcribed from total RNA using iScript Reverse Transcriptase kit (Bio-Rad). For determination of isoform ratio between differentiation, cDNA was amplified with DreamTaq Green PCR Master Mix (ThermoFisher) and visualized on a 2% agarose gel in the presence of SYBR Safe (Invitrogen). For qRT-PCR, PCR amplification reactions were performed with iTaq Universal SYBR Green Supermix (Bio-Rad). Reactions were carried out on a CFX Opus 384 Real-Time PCR System (Bio-Rad). Gene expression analysis was performed using the $2^{-\Delta\Delta Ct}$ method. The specific primers used are listed in Table S6.

RNA sequencing

Total RNA was subjected to library preparation and RNA sequencing by BGI Americas (Cambridge, MA) using the BGISEQ-500 sequencing platform with 150 bp paired-end reads. The raw reads were aligned to the reference genome hg38 using STAR aligner (version 2.7.4a) with default parameters. NCBI RefSeq hg38 was used for gene annotation. Reads falling in genes were counted using featureCounts (version 2.0.1) with the parameters '-p -B -t exon' and differential analysis was performed with DESeq2 (version 1.34.0) with default parameters. Log2(FC) was calculated by subtracting log2-transformed mean counts in each group. Genes with p value <0.01 and |log2(FC)| > 1 were considered differentially expressed.

Alternative splicing events analysis

RNA-sequencing of normal keratinocytes (n = 3 each) was assessed with rMATS (version 3.2.5) to identify differential exon usage. Significant alternative splicing events were defined as exons displaying a difference in the percentage spliced in (PSI) between progenitor and differentiated of at least 0.1 and having a false discovery rate (FDR) below 0.05.

Flow sort experiment

An adult male human skin sample was collected from a discarded surgical specimen taken from the trunk, collected upon written informed consent under an institutional review board protocol approved by the University of California, San Diego. The sample was free from signs of visible sun damage or skin disease. Tissues were macro dissected to remove the subcutaneous fat layer then treated with dispase at 4°C for 12 h. The epidermis was mechanically separated from the dermis and dissociated in 0.05% trypsin for 15 min. Dissociated epidermal keratinocytes were isolated, counted, and labeled with a phycoerythrin-conjugated integrin beta 4 antibody (Santa Cruz, sc-13543) using 2 μg antibody per million cells for 2 h, then washed three times with ice-cold DPBS Sorting Buffer (1X DPBS, 20 mM HEPES pH 7.2, 1% BSA). Keratinocytes were sorted on a BD Biosciences FACSAriaIII instrument into Trizol-LS media, with total RNA from ITGB4-high and ITGB4-negative cells (Figure S1) isolated according to manufacturer's recommended protocol.

RNA immunoprecipitation

RNA immunoprecipitation was performed with the Magna RIP RNA-Binding Protein Immunoprecipitation Kit (Millipore Sigma, catalog # 17–700) following the manufacturer's instructions. For each assay, 2.5 x 10^6 primary human keratinocytes were used. For each immunoprecipitation, 3–5 μg of negative control IgG or experimental antibody against SRSF1 (Thermo Fisher, cat. # 32–4500), TARDBP (Cell Signaling Technology, cat. # 3448S), or FUS (Cell Signaling Technology, cat. # 67840S) was used. RNA was extracted and purified with phenol/chloroform then subjected to RT-qPCR and RT-PCR analysis.

Protein isolation and immunoblot

Keratinocytes were washed with cold phosphate-buffered saline (PBS), and protein lysates were extracted with RIPA buffer supplemented with protease inhibitor cocktail (Roche). Protein quantification was performed with the BCA Assay kit (Pierce). Proteins were analyzed using western blotting. Protein lysates were loaded onto 4–12% Bis-Tris gels (Invitrogen) and resolved by electrophoresis using Bolt MOPS SDS Running buffer (Invitrogen). Wet transfer was performed onto PVDF membranes, and primary antibodies were incubated overnight at 4°C. Membranes were washed three times in PBS-0.1% Tween then incubated with fluorescent secondary antibodies according to manufacturer's recommendations (Li-Cor), washed and visualized. Blots were imaged on an Odyssey imager (Li-Cor). Quantification was performed using Image Studio software (LI-COR Biosciences). The antibodies used are listed in Key Resources Table.

siRNA transfection

Keratinocytes were seeded onto 6 well plates at 2.5 × 10^5 cells per well for 24 h. Cells were transfected with small interfering RNA (siRNA; 10 μmol/L) using Lipofectamine RNAiMax (Invitrogen) following the recommended manufacturer's protocol. The knockdown efficiency was assessed using real-time PCR and Western blot.

MAP3K7 long and short isoform overexpression

The plasmids pcDNA3.1-C-(k)DYK-MAP3K7 long (Genescript, cat. #OHu21832) and short (Genescript, cat. #OHu14588) were used to overexpress each isoform. Keratinocytes were seeded onto 12 well plates at 1.5 × 10^5 cells for 24 h. Cells were transfected with each plasmids using Attractene Transfection Reagent (Qiagen). For each transfection, 600ng of each plasmid was added to EpiLife medium (Thermo Fisher Scientific) for a total of 60μL, and mixed with 2.25μL Attractene. Transfection mixtures were incubated for 15 min at room temperature to allow complex formation. The Attractene-plasmid mixtures were then added to each well dropwise and swirled. The assay outputs were assessed by real-time PCR and Western blot.

NF-κB ELISA

Cells were washed with ice-cold PBS with phosphatase inhibitor and nuclear extracts prepared using the Nuclear Extract Kit (Active Motif) according to the manufacturer's protocol. NF-κB activity was measured using equal amounts of nuclear protein extracts by the TransAM NF-κB p65 kit (Active Motif), an ELISA-based kit to detect and quantify NF-κB p65 subunit activation. The assay was performed according to the manufacturer's protocol. Results for the chemiluminescent TransAM kit were analyzed using a SpectraMax iD3 (Molecular Devices).

Immunofluorescence of organotypic cultures

Organotypic culture sections were fixed in 4% PFA. Sections were blocked in 5% normal goat serum for 1 h at room temperature, then labeled with primary antibodies diluted in TBS-T overnight at 4°C. After washing three times in TBS-T, sections were incubated with secondary antibodies for 1 h at room temperature. Slides were washed three times in TBS-T, incubated for 1 min in Hoescht stain to label nuclei, washed in TBS two times, then mounted with Prolong Gold (Thermo Fisher) and coverslips. The primary and secondary

antibodies used are listed in Key Resources Table. Epidermal thickness was measured at three fixed sites across the tissue using ImageJ, measured from the basement membrane to the most superficial aspect of the stratum corneum. The percentage of KI67-positive cells was counted using ImageJ using Analyze particles feature on both DAPI-positive and KI67-positive cells. For quantification of KRT10, the total (Hoechst and KRT10) and KRT10 fluorescent signals were quantified using ImageJ (''Threshold color'' and ''Measure'' features), and the %KRT10 was measured as the ratio of the KRT10 signal (''area'') over the total fluorescent signal.

QUANTIFICATION AND STATISTICAL ANALYSIS

Band quantitation

Intensity of bands was quantitated with Image Lab Software analysis (Bio-Rad). Channel lanes and bands in the agarose gel were detected using default software parameters and verified visually. Quantitation was performed using default software settings. Relative quantitation of bands was denoted in the paper as the proportion of the intensity of the largest isoform relative to the sum of intensities of all isoforms (percentage spliced in).

Statistical analysis

Data are presented as the mean ± standard deviation (SD) or standard error (SEM). For experiments reporting SEM, replicates are primary epidermal keratinocytes derived from distinct biological donors. For two group comparisons, statistical analysis for significance was determined using student t-test with a threshold of $p \leq 0.05$ considered to be significant. For comparisons involving three or more groups, statistical analysis for significance was determined using one-way ANOVA with a Tukey's HSD post hoc test with a threshold of $p \leq 0.05$ considered to be significant. GraphPad Prism 9 (GraphPad Software) was used to execute statistical comparisons. The details of statistical analysis are indicated in the figure legends.